Exploring Synchronization in Complex Oscillator Networks

Florian Dörfler   Francesco Bullo

***Abstract*— The emergence of synchronization in a network of coupled oscillators is a pervasive topic in various scientific disciplines ranging from biology, physics, and chemistry to social networks and engineering applications. A coupled oscillator network is characterized by a population of heterogeneous oscillators and a graph describing the interaction among the oscillators. These two ingredients give rise to a rich dynamic behavior that keeps on fascinating the scientific community. In this article, we present a tutorial introduction to coupled oscillator networks, we review the vast literature on theory and applications, and we present a collection of different synchronization notions, conditions, and analysis approaches. We focus on the canonical phase oscillator models occurring in countless real-world synchronization phenomena, and present their rich phenomenology. We review a set of applications relevant to control scientists. We explore different approaches to phase and frequency synchronization, and we present a collection of synchronization conditions and performance estimates. For all results we present self-contained proofs that illustrate a sample of different analysis methods in a tutorial style.**

I. INTRODUCTION

The scientific interest in synchronization of coupled oscillators can be traced back to the work by Christiaan Huygens on "an odd kind sympathy" between coupled pendulum clocks [1], and it still fascinates the scientific community nowadays [2], [3]. Within the rich modeling phenomenology on synchronization among coupled oscillators, we focus on the canonical model of a continuous-time limit-cycle oscillator network with continuous and bidirectional coupling.

A network of coupled phase oscillators: A mechanical analog of a coupled oscillator network is the spring network shown in Figure 1 and consists of a group of kinematic particles constrained to rotate around a circle and assumed to move without colliding. Each particle is characterized by a phase angle $\theta_i \in \mathbb{S}^1$ and has a preferred natural rotation frequency $\omega_i \in \mathbb{R}$. Pairs of interacting particles i and j are coupled through an elastic spring with stiffness $a_{ij} > 0$. We refer to [4] for a first principle modeling of the spring-interconnected particles depicted in Figure 1.

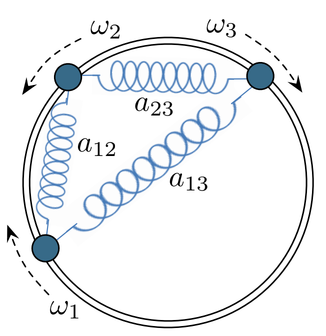

Fig. 1. Mechanical analog of a coupled oscillator network

This material is based in part upon work supported by NSF grants IIS-0904501 and CPS-1135819.

Florian Dörfler and Francesco Bullo are with the Center for Control, Dynamical Systems and Computation, University of California at Santa Barbara. Email: {dorfler,bullo}@engineering.ucsb.edu

Formally, each isolated particle is an oscillator with first-order dynamics $\dot{\theta}_i = \omega_i$. The interaction among n such oscillators is modeled by a connected graph $G(\mathcal{V}, \mathcal{E}, A)$ with nodes $\mathcal{V} = \{1, \dots, n\}$, edges $\mathcal{E} \subset \mathcal{V} \times \mathcal{V}$, and positive weights $a_{ij} > 0$ for each undirected edge $\{i, j\} \in \mathcal{E}$. Under these assumptions, the overall dynamics of the coupled oscillator network are

$$\dot{\theta}_i = \omega_i - \sum\nolimits_{j=1}^{n} a_{ij} \sin(\theta_i - \theta_j) \,, \qquad i \in \{1, \dots, n\} \,. \quad (1)$$

The rich dynamic behavior of the coupled oscillator model (1) arises from a competition between each oscillator's tendency to align with its natural frequency ω_i and the synchronization-enforcing coupling $a_{ij}\sin(\theta_i - \theta_j)$ with its neighbors. Intuitively, a weakly coupled and strongly heterogeneous network does not display any coherent behavior, whereas a strongly coupled and sufficiently homogeneous network is amenable to synchronization, where all frequencies $\dot{\theta}_i(t)$ or even all phases $\theta_i(t)$ become aligned.

History, applications and related literature: The coupled oscillator model (1) has first been proposed by Arthur Winfree [5]. In the case of a complete interaction graph, the coupled oscillator dynamics (1) are nowadays known as the *Kuramoto model* of coupled oscillators due to Yoshiki Kuramoto [6], [7]. Stephen Strogatz provides an excellent historical account in [8]. We also recommend the survey [9].

Despite its apparent simplicity, the coupled oscillator model (1) gives rise to rich dynamic behavior. This model is encountered in various scientific disciplines ranging from natural sciences over engineering applications to social networks. The model and its variations appear in the study if biological synchronization phenomena such as pacemaker cells in the heart [10], circadian rhythms [11], neuroscience [12]–[14], metabolic synchrony in yeast cell populations [15], flashing fireflies [16], chirping crickets [17], biological locomotion [18], animal flocking behavior [19], fish schools [20], and rhythmic applause [21], among others. The coupled oscillator model (1) also appears in physics and chemistry in modeling and analysis of spin glass models [22], [23], flavor evolutions of neutrinos [24], coupled Josephson junctions [25], and in the analysis of chemical oscillations [26].

Some technological applications of the coupled oscillator model (1) include deep brain stimulation [27], [28], vehicle coordination [20], [29]–[32], carrier synchronization without phase-locked loops [33], semiconductor lasers [34], [35], microwave oscillators [36], clock synchronization in decentralized computing networks [37]–[42], decentralized maximum likelihood estimation [43], and droop-controlled inverters in microgrids [44]. Finally, the coupled oscillator model (1) also serves as the prototypical example for synchronization in complex networks [45]–[48] and its linearization is the well-known consensus protocol studied in networked control, see the surveys and monographs [49]–[51]. Various control scientists explored the coupled oscillator model (1) as a nonlinear generalization of the consensus protocol [52]–[58].

Second-order variations of the coupled oscillator model (1) appear in synchronization phenomena, in population of flashing fireflies [59], in particle models mimicking animal flocking behavior [60], [61], in structure-preserving power system models, [62], [63] in network-reduced power system models [64], [65], in coupled metronomes [66], in pedestrian crowd synchrony on London's Millennium bridge [67], and in Huygen's pendulum coupled clocks [68]. Coupled oscillator networks with second-order dynamics have been theoretically analyzed in [9], [69]–[75], among others.

Coupled oscillator models of the form (1) are also studied from a purely theoretic perspective in the physics, dynamical systems, and control communities. At the heart of the coupled oscillator dynamics is the transition from incoherence to synchrony. Here, different notions and degrees of synchronization can be distinguished [75]–[77], and the (apparently) incoherent state features rich and largely unexplored dynamics as well [48], [78]–[80]. In this article we will be particularly interested in phase and frequency synchronization when all phases $\theta_i(t)$ become aligned, respectively all frequencies $\dot{\theta}_i(t)$ become aligned. We refer to [4], [8], [9], [20], [29], [32], [53], [54], [57], [65], [69], [75]–[77], [81]–[111] for an incomplete overview concerning numerous recent research activities. We will review some of this literature throughout the paper and refer to the surveys [8], [9], [45]–[47], [75] for further applications and numerous theoretic results concerning the coupled oscillator model (1).

Contributions and contents: In this paper, we introduce the reader to synchronization in networks of coupled oscillators. We present a sample of important analysis concepts in a tutorial style and from a control-theoretic perspective.

In Section II, we will review a set of selected technological applications which are directly tied to the coupled oscillator model (1) and also relevant to control systems. We will cover vehicle coordination and electric power networks in depth, and also justify the importance of (1) as a canonical model. Prompted by these applications, we review the existing results concerning phase synchronization, phase balancing, and frequency synchronization, and we also present some novel results on synchronization in sparsely-coupled networks.

Section III introduces the reader to different synchronization notions, performance metrics, and synchronization conditions. Section IV presents a collection of important results regarding phase synchronization, phase balancing, and frequency synchronization. By now the analysis methods for synchronization have reached a mature level, and we present simple and self-contained proofs using a sample of different analysis methods. In particular, we present one result on phase synchronization and one result on phase balancing including estimates on the exponential synchronization rate and the region of attraction (see Theorem 4.3 and Theorem 4.4). We also present some implicit and explicit, and necessary and sufficient conditions for frequency synchronization in the classic homogeneous case of a complete and uniformly-weighted coupling graphs (see Theorem 4.5). Concerning frequency synchronization in sparse graphs, we present two partially new synchronization conditions depending on the algebraic connectivity (see Theorem 4.6 and Theorem 4.7).

Finally, Section V concludes the paper. We summarize the limitations of existing analysis methods and suggest some important directions for future research.

Preliminaries and notation: The remainder of this section introduces some notation and recalls some preliminaries.

Vectors and functions: Let $\mathbf{1}_n$ and $\mathbf{0}_n$ be the n-dimensional vector of unit and zero entries, and let $\mathbf{1}_n^\perp$ be the orthogonal complement of $\mathbf{1}_n$ in $\mathbb{R}^n$, that is, $\mathbf{1}_n^\perp \triangleq \{x \in \mathbb{R}^n : x \perp \mathbf{1}_n\}$. Given an n-tuple $(x_1, \dots, x_n)$, let $x \in \mathbb{R}^n$ be the associated vector with maximum and minimum elements x_{max} and x_{min}. For an ordered index set $\mathcal{I}$ of cardinality $|\mathcal{I}|$ and an one-dimensional array $\{x_i\}_{i\in\mathcal{I}}$, let $\operatorname{diag}(\{c_i\}_{i\in\mathcal{I}}) \in \mathbb{R}^{|\mathcal{I}|\times|\mathcal{I}|}$ be the associated diagonal matrix. Finally, define the continuous function $\operatorname{sinc} : \mathbb{R} \to \mathbb{R}$ by $\operatorname{sinc}(x) = \sin(x)/x$ for $x \neq 0$.

Geometry on the n-torus: The set $\mathbb{S}^1$ denotes the *unit circle*, an *angle* is a point $\theta \in \mathbb{S}^1$, and an *arc* is a connected subset of $\mathbb{S}^1$. The *geodesic distance* between two angles $\theta_1, \theta_2 \in \mathbb{S}^1$ is the minimum of the counter-clockwise and the clockwise arc lengths connecting θ_1 and θ_2. With slight abuse of notation, let $|\theta_1 - \theta_2|$ denote the *geodesic distance* between two angles $\theta_1, \theta_2 \in \mathbb{S}^1$. The *$n$-torus* is the product set $\mathbb{T}^n = \mathbb{S}^1 \times \cdots \times \mathbb{S}^1$ is the direct sum of n unit circles. For $\gamma \in [0, 2\pi[$, let $\overline{\operatorname{Arc}}_n(\gamma) \subset \mathbb{T}^n$ be the closed set of angle arrays $\theta = (\theta_1, \dots, \theta_n)$ with the property that there exists an arc of length γ containing all $\theta_1, \dots, \theta_n$. Thus, an angle array $\theta \in \overline{\operatorname{Arc}}_n(\gamma)$ satisfies $\max_{i,j\in\{1,\dots,n\}} |\theta_i - \theta_j| \leq \gamma$. Finally, let $\operatorname{Arc}_n(\gamma)$ be the interior of the set $\overline{\operatorname{Arc}}_n(\gamma)$.

Algebraic graph theory: Let $G(\mathcal{V}, \mathcal{E}, A)$ be an undirected, connected, and weighted graph without self-loops. Let $A \in \mathbb{R}^{n\times n}$ be its symmetric nonnegative *adjacency matrix* with zero diagonal, $a_{ii} = 0$. For each node $i \in \{1, \dots, n\}$, define the nodal degree by $\deg_i = \sum_{j=1}^n a_{ij}$. Let $L \in \mathbb{R}^{n\times n}$ be the *Laplacian matrix* defined by $L = \operatorname{diag}(\{\deg_i\}_{i=1}^n) - A$. If a number $\ell \in \{1, \dots, |\mathcal{E}|\}$ and an arbitrary direction is assigned to each edge $\{i, j\} \in \mathcal{E}$, the (oriented) *incidence matrix* $B \in \mathbb{R}^{n\times|\mathcal{E}|}$ is defined component-wise by $B_{k\ell} = 1$ if node k is the sink node of edge ℓ and by $B_{k\ell} = -1$ if node k is the source node of edge ℓ; all other elements are zero. For $x \in \mathbb{R}^n$, the vector $B^T x$ has components $x_i - x_j$ corresponding to the oriented edge from j to i, that is, B^T maps node variables x_i, x_j to incremental edge variables $x_i - x_j$. If $\operatorname{diag}(\{a_{ij}\}_{\{i,j\}\in\mathcal{E}})$ is the diagonal matrix of edge weights, then $L = B \operatorname{diag}(\{a_{ij}\}_{\{i,j\}\in\mathcal{E}}) B^T$. If the graph is connected, then $\operatorname{Ker}(B^T) = \operatorname{Ker}(L) = \operatorname{span}(\mathbf{1}_n)$, all $n - 1$ non-zero eigenvalues of L are strictly positive, and the second-smallest eigenvalue $\lambda_2(L)$ is called the *algebraic connectivity* and is a spectral connectivity measure.

II. Applications of the Coupled Oscillator Model Relevant to Control Systems

Here, we detail a set of selected technological applications which are relevant to control systems scientists.

A. Flocking, Schooling, and Planar Vehicle Coordination

An emerging research field in control is the coordination of autonomous vehicles based on locally available information and inspired by biological flocking phenomena. Consider a set of n particles in the plane $\mathbb{R}^2$, which we identify with the complex plane $\mathbb{C}$. Each particle $i \in \mathcal{V} = \{1, \dots, n\}$ is characterized by its position $r_i \in \mathbb{C}$, its heading angle $\theta_i \in \mathbb{S}^1$, and a steering control law $u_i(r, \theta)$ depending on the position and heading of itself and other vehicles. For simplicity, we assume that all particles have constant and unit speed. The particle kinematics are then given by [112]

$$\left.\begin{aligned} \dot{r}_i &= e^{\mathrm{i}\theta_i}\,, \\ \dot{\theta}_i &= u_i(r,\theta)\,, \end{aligned}\right\} \quad i \in \{1, \dots, n\}\,, \tag{2}$$

where $\mathrm{i} = \sqrt{-1}$ is the imaginary unit. If the control u_i is identically zero, then particle i travels in a straight line with orientation $\theta_i(0)$, and if $u_i = \omega_i \in \mathbb{R}$ is a nonzero constant, then the particle traverses a circle with radius $1/|\omega_i|$.

The interaction among the particles is modeled by a possibly time-varying interaction graph $G(\mathcal{V}, \mathcal{E}(t), A(t))$ determined by communication and sensing patterns. Some interesting motion patterns emerge if the controllers use only relative phase information between neighboring particles, that is, $u_i = \omega_0(t) + f_i(\theta_i - \theta_j)$ for $\{i, j\} \in \mathcal{E}(t)$ and $\omega_0 : \mathbb{R}_{\geq 0} \to \mathbb{R}$. For example, the control $u_i = \omega_0(t) - K \cdot \sum_{j=1}^{n} a_{ij}(t) \sin(\theta_i - \theta_j)$ with gain $K \in \mathbb{R}$ results in

$$\dot{\theta}_i = \omega_0(t) - K \cdot \sum\nolimits_{j=1}^{n} a_{ij}(t) \sin(\theta_i - \theta_j)\,, \quad i \in \mathcal{V}\,. \tag{3}$$

The controlled phase dynamics (3) correspond to the coupled oscillator model (1) with a time-varying interaction graph with weights $K \cdot a_{ij}(t)$ and identically time-varying natural frequencies $\omega_i = \omega_0(t)$ for all $i \in \{1, \dots, n\}$. The controlled phase dynamics (3) give rise to very interesting coordination patterns that mimic animal flocking behavior [19] and fish schools [20]. Inspired by these biological phenomena, the controlled phase dynamics (3) and its variations have also been studied in the context of tracking and formation controllers in swarms of autonomous vehicles [20], [29]–[32]. A few trajectories are illustrated in Figure 2, and we refer to [20], [29]–[32] for other control laws and motion patterns.

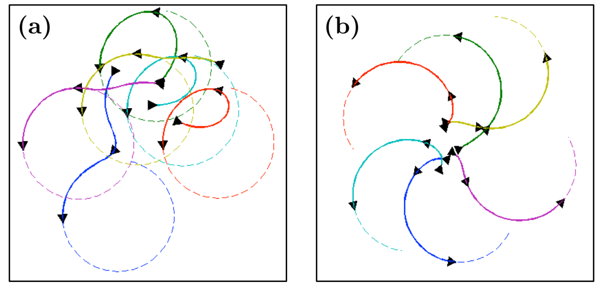

Fig. 2. Illustration of the controlled dynamics (2)-(3) with $n = 6$ particles, a complete interaction graph, and identical and constant natural frequencies $\omega_0(t) = 1$, where $K = 1$ in panel (a) and $K = -1$ in panel (b). The arrows depict the orientation, the dashed curves show the long-term position dynamics, and the solid curves show the initial transient position dynamics. It can be seen that even for this simple choice of controller, the resulting motion results in "synchronized" or "balanced" heading angles for $K = \pm 1$.

In the following sections, we will present various tools to analyze the motion patterns in Figure 2, which we will refer to as *phase synchronization* and *phase balancing*.

B. Power Grids with Synchronous Generators and Inverters

Here, we present the *structure-preserving power network model* introduced in [62] and refer to [63, Chapter 7] for detailed derivation from a higher order first principle model. Additionally, we equip the power network model with a set of inverters and refer to [44] for a detailed modeling.

Consider an alternating current (AC) power network modeled as an undirected, connected, and weighted graph with node set $\mathcal{V} = \{1, \dots, n\}$, transmission lines $\mathcal{E} \subset \mathcal{V} \times \mathcal{V}$, and admittance matrix $Y = Y^T \in \mathbb{C}^{n \times n}$. For each node, consider the voltage phasor $V_i = |V_i| e^{\mathrm{i}\theta_i}$ corresponding to the phase $\theta_i \in \mathbb{S}^1$ and magnitude $|V_i| \geq 0$ of the sinusoidal solution to the circuit equations. If the network is lossless, then the active power flow from node i to j is $a_{ij} \sin(\theta_i - \theta_j)$, where we used the shorthand $a_{ij} = |V_i| \cdot |V_j| \cdot \Im(Y_{ij})$.

In the following, we assume that the node set is partitioned as $\mathcal{V} = \mathcal{V}_1 \cup \mathcal{V}_2 \cup \mathcal{V}_3$, where $\mathcal{V}_1$ are load buses, $\mathcal{V}_2$ are conventional synchronous generators, and $\mathcal{V}_3$ are grid-connected direct current (DC) power sources, such as solar farms. The active power drawn by a load $i \in \mathcal{V}_1$ consists of a constant term $P_{\mathrm{l},i} > 0$ and a frequency-dependent term $D_i \dot{\theta}_i$ with $D_i > 0$. The resulting power balance equation is

$$D_i \dot{\theta}_i + P_{\mathrm{l},i} = -\sum\nolimits_{j=1}^{n} a_{ij} \sin(\theta_i - \theta_j)\,, \quad i \in \mathcal{V}_1\,. \tag{4}$$

If the generator reactances are absorbed into the admittance matrix, then the swing dynamics of generator $i \in \mathcal{V}_2$ are

$$M_i \ddot{\theta}_i + D_i \dot{\theta}_i = P_{\mathrm{m},i} - \sum\nolimits_{j=1}^{n} a_{ij} \sin(\theta_i - \theta_j)\,, \quad i \in \mathcal{V}_2, \tag{5}$$

where $\theta_i \in \mathbb{S}^1$ and $\dot{\theta}_i \in \mathbb{R}^1$ are the generator rotor angle and frequency, $P_{\mathrm{m},i} > 0$ is the mechanical power input, and $M_i > 0$, and $D_i > 0$ are the inertia and damping coefficients.

We assume that each DC source is connected to the AC grid via an DC/AC inverter, the inverter output impendances are absorbed into the admittance matrix, and each inverter is equipped with a conventional droop-controller. For a droop-controlled inverter $i \in \mathcal{V}_3$ with droop-slope $1/D_i > 0$, the deviation of the power output $\sum_{j=1}^{n} a_{ij} \sin(\theta_i - \theta_j)$ from its nominal value $P_{\mathrm{d},i} > 0$ is proportional to the frequency deviation $D_i \dot{\theta}_i$. This gives rise to the inverter dynamics

$$D_i \dot{\theta}_i = P_{\mathrm{d},i} - \sum\nolimits_{j=1}^{n} a_{ij} \sin(\theta_i - \theta_j)\,, \quad i \in \mathcal{V}_3\,. \tag{6}$$

These power network devices are illustrated in Figure 3. Finally, we remark that different load models such as constant power/current/susceptance loads and synchronous motor loads can be modeled and analyzed by the same set of equations (4)-(6), see [63]–[65], [113], [114].

Synchronization is pervasive in the operation of power networks. All generating units of an interconnected grid must

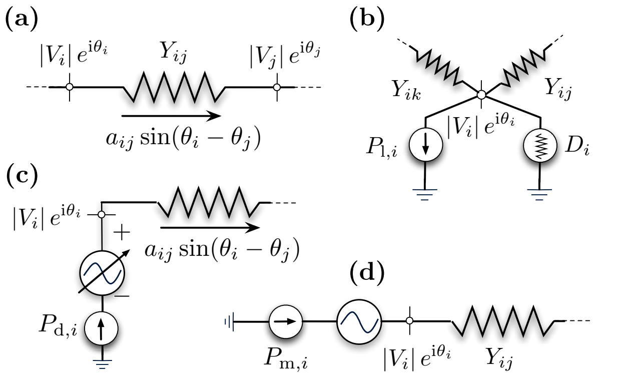

Fig. 3. Illustration of the power network devices as circuit elements. Subfigure (a) shows a transmission element connecting nodes i and j, Subfigure (b) shows a frequency-dependent load, Subfigure (c) shows an inverter controlled according to (6), and Subfigure (d) shows a synchronous generator.

remain in strict frequency synchronism while continuously following demand and rejecting disturbances. Notice that, with exception of the inertial terms $M_i\ddot{\theta}_i$ and the possibly non-unit coefficients D_i, the power network dynamics (4)-(6) are a perfect electrical analog of the coupled oscillator model (1) with $\omega = (-P_{\mathrm{l},i}, P_{\mathrm{m},i}, P_{\mathrm{d},i})$. Thus, it is not surprising that scientists from different disciplines recently advocated coupled oscillator approaches to analyze synchronization in power networks [4], [44], [65], [70], [97], [115]–[119].

The theoretic tools presented in the following sections establish how *frequency synchronization* in power networks depend on the nodal parameters $(P_{\mathrm{l},i}, P_{\mathrm{m},i}, P_{\mathrm{d},i})$ as well as the interconnecting electrical network with weights a_{ij}.

C. Canonical Coupled Oscillator Model

The importance of the coupled oscillator model (1) does not stem only from the various examples listed in Sections I and II. Even though model (1) appears to be quite specific (a phase oscillator with constant driving term and continuous, diffusive, and sinusoidal coupling), it is the *canonical model* of coupled limit-cycle oscillators [120]. In the following, we briefly sketch how such general models can be reduced to model (1). We schematically follow the approaches [121, Chapter 10], [122] developed in the computational neuroscience community without aiming at mathematical precision, and we refer to [120], [123] for further details.

Consider an oscillator modeled as a dynamical system with state $x \in \mathbb{R}^m$ and nonlinear dynamics $\dot{x} = f(x)$, which admit a locally exponentially stable periodic orbit $\gamma \subset \mathbb{R}^m$ with period $T > 0$. By a change of variables, any trajectory in a local neighborhood of γ can be characterized by a phase variable $\varphi \in \mathbb{S}^1$ with dynamics $\dot{\varphi} = \Omega$, where $\Omega = 2\pi/T$.

Now consider n such limit cycle oscillators, where $x_i \in \mathbb{R}^m$ is the state of oscillator i with limit cycle $\gamma_i \subset \mathbb{R}^m$ and period $T_i > 0$. We assume that the oscillators are weakly coupled with interaction graph $G(\mathcal{V},\mathcal{E})$ and dynamics

$$\dot{x}_i = f_i(x_i) + \epsilon \sum\nolimits_{\{i,j\}\in\mathcal{E}} g_{ij}(x_i,x_j)\,,\quad i \in \{1,\dots,n\}\,, \quad (7)$$

where $\epsilon > 0$ and $g_{ij}(\cdot)$ is the coupling function for the pair $\{i,j\} \in \mathcal{E}$. The coupling $g_{ij}(\cdot)$ can possibly be impulsive. For sufficiently weak coupling constant ϵ, the attractive limit cycles γ_i persist, and the phase dynamics are obtained as

$$\dot{\varphi}_i = \Omega_i + \epsilon \sum\nolimits_{\{i,j\}\in\mathcal{E}} Q_i(\varphi) g_{ij}(x_i(\varphi_i), x_j(\varphi_j))\,,$$

where $Q_i(\varphi)$ is the infinitesimal phase response curve (or linear response function) associated with oscillator i, $\Omega_i = 2\pi/T_i$, and we dropped higher order terms of order $\mathcal{O}(\epsilon^2)$.

The local change of variables $\theta_i(t) = \varphi_i(t) - \Omega_i t$ yields

$$\dot{\theta}_i = \epsilon \sum\nolimits_{\{i,j\}\in\mathcal{E}} Q_i(\theta_i + \Omega_i t) g_{ij}(x_i(\theta_i + \Omega_i t), x_j(\theta_j + \Omega_j t)).$$

An averaging analysis applied to the θ-dynamics results in

$$\dot{\theta}_i = \epsilon\omega_i + \epsilon \sum\nolimits_{\{i,j\}\in\mathcal{E}} h_{ij}(\theta_i - \theta_j)\,, \quad (8)$$

where $\omega_i = h_{ii}(0)$ and the averaged coupling functions are

$$h_{ij}(\chi) = \lim_{T\to\infty} \frac{1}{T}\int_0^T Q_i(\Omega_i\tau) g_{ij}(x_i(\Omega_i\tau), x_j(\Omega_j\tau - \chi))d\tau.$$

Notice that the averaged coupling functions h_{ij} are 2π-periodic and the coupling is diffusive. If all functions h_{ij} are odd, a first-order Fourier series expansion of h_{ij} yields $h_{ij}(\cdot) \approx a_{ij}\sin(\cdot)$ as first harmonic with some coefficient a_{ij}. In this case, the dynamics (8) in the slow time scale $\tau = \epsilon t$ reduce exactly to the coupled oscillator model (1).

This analysis justifies calling the coupled oscillator model (1) the *canonical model* for coupled limit-cycle oscillators.

III. Synchronization Notions and Metrics

In this section, we introduce different notions of synchronization. Whereas the first four subsections address the commonly studied notions of synchronization associated with a coherent behavior and cohesive phases, Subsection III-D addresses the converse concept of phase balancing.

A. Synchronization Notions

The coupled oscillator model (1) evolves on $\mathbb{T}^n$, and features an important symmetry, namely the rotational invariance of the angular variable θ. This symmetry gives rise to the rich synchronization dynamics. Different levels of synchronization can be distinguished, and the most commonly studied notions are phase and frequency synchronization.

Phase synchronization: A solution $\theta : \mathbb{R}_{\geq 0} \to \mathbb{T}^n$ to the coupled oscillator model (1) achieves *phase synchronization* if all phases $\theta_i(t)$ become identical as $t \to \infty$.

Phase cohesiveness: As we will see later, phase synchronization can occur only if all natural frequencies ω_i are identical. If the natural frequencies are not identical, then each pairwise distance $|\theta_i(t) - \theta_j(t)|$ can converge to a constant but not necessarily zero value. The concept of phase cohesiveness formalizes this possibility. For $\gamma \in [0,\pi[$, let $\bar{\Delta}_G(\gamma) \subset \mathbb{T}^n$ be the closed set of angle arrays $(\theta_1,\dots,\theta_n)$ with the property $|\theta_i - \theta_j| \leq \gamma$ for all $\{i,j\} \in \mathcal{E}$, that is, each pairwise phase distance is bounded by γ. Also, let $\Delta_G(\gamma)$ be the interior of $\bar{\Delta}_G(\gamma)$. Notice that $\overline{\mathrm{Arc}}_n(\gamma) \subseteq \bar{\Delta}_G(\gamma)$ but the two sets are generally not equal. A solution $\theta : \mathbb{R}_{\geq 0} \to \mathbb{T}^n$ is then said to be *phase cohesive* if there exists a length $\gamma \in [0,\pi[$ such that $\theta(t) \in \bar{\Delta}_G(\gamma)$ for all $t \geq 0$.

Frequency synchronization: A solution $\theta : \mathbb{R}_{\geq 0} \to \mathbb{T}^n$ achieves *frequency synchronization* if all frequencies $\dot{\theta}_i(t)$ converge to a common frequency $\omega_{\text{sync}} \in \mathbb{R}$ as $t \to \infty$. The explicit synchronization frequency $\omega_{\text{sync}} \in \mathbb{R}$ of the coupled oscillator model (1) can be obtained by summing over all equations in (1) as $\sum_{i=1}^n \dot{\theta}_i = \sum_{i=1}^n \omega_i$. In the frequency-synchronized case, this sum simplifies to $\sum_{i=1}^n \omega_{\text{sync}} = \sum_{i=1}^n \omega_i$. In conclusion, if a solution of the coupled oscillator model (1) achieves frequency synchronization, then it does so with synchronization frequency equal to $\omega_{\text{sync}} = \sum_{i=1}^n \omega_i/n$. By transforming to a rotating frame with frequency ω_{sync} and by replacing ω_i by $\omega_i - \omega_{\text{sync}}$, we obtain $\omega_{\text{sync}} = 0$ (or equivalently $\omega \in \mathbf{1}_n^\perp$). In what follows, without loss of generality, we will sometimes assume that $\omega \in \mathbf{1}_n^\perp$ so that $\omega_{\text{sync}} = 0$.

*Remark 1 (***Terminology***):* Alternative terminologies for phase synchronization include full, exact, or perfect synchronization. For a frequency-synchronized solution all phase distances $|\theta_i(t) - \theta_j(t)|$ are constant in a rotating coordinate frame with frequency ω_{sync}, and the terminology *phase locking* is sometimes used instead of frequency synchronization. Other commonly used terms include frequency locking, frequency entrainment, or also partial synchronization. □

Synchronization: The main object under study in most applications and theoretic analyses are phase cohesive and frequency-synchronized solutions, that is, all oscillators rotate with the same synchronization frequency, and all their pairwise phase distances are bounded. In the following, we restrict our attention to synchronized solutions with sufficiently small phase distances $|\theta_i - \theta_j| \leq \gamma < \pi/2$ for $\{i,j\} \in \mathcal{E}$. Of course, there may exist other possible solutions, but these are not necessarily stable (see our analysis in Section IV) or not relevant in most applications[1]. We say that a solution $\theta : \mathbb{R}_{\geq 0} \to \mathbb{T}^n$ to the coupled oscillator model (1) is *synchronized* if there exists $\theta_{\text{sync}} \in \bar{\Delta}_G(\gamma)$ for some $\gamma \in [0, \pi/2[$ and $\omega_{\text{sync}} \in \mathbb{R}$ (identically zero for $\omega \in \mathbf{1}_n^\perp$) such that $\theta(t) = \theta_{\text{sync}} + \omega_{\text{sync}} \mathbf{1}_n t \pmod{2\pi}$ for all $t \geq 0$.

Synchronization manifold: The geometric object under study in synchronization is the synchronization manifold. Given a point $r \in \mathbb{S}^1$ and an angle $s \in [0, 2\pi]$, let $\text{rot}_s(r) \in \mathbb{S}^1$ be the rotation of r counterclockwise by the angle s. For $(r_1, \ldots, r_n) \in \mathbb{T}^n$, define the equivalence class

$$[(r_1, \ldots, r_n)] = \{(\text{rot}_s(r_1), \ldots, \text{rot}_s(r_n)) \in \mathbb{T}^n \,|\, s \in [0, 2\pi]\}.$$

Clearly, if $(r_1, \ldots, r_n) \in \bar{\Delta}_G(\gamma)$ for some $\gamma \in [0, \pi/2[$, then $[(r_1, \ldots, r_n)] \subset \bar{\Delta}_G(\gamma)$. Given a synchronized solution characterized by $\theta_{\text{sync}} \in \bar{\Delta}_G(\gamma)$ for some $\gamma \in [0, \pi/2[$, the set $[\theta_{\text{sync}}] \subset \bar{\Delta}_G(\gamma)$ is a *synchronization manifold* of the coupled-oscillator model (1). Note that a synchronized solution takes value in a synchronization manifold due to rotational symmetry, and for $\omega \in \mathbf{1}_n^\perp$ (implying $\omega_{\text{sync}} = 0$) a synchronization manifold is also an equilibrium manifold of the coupled oscillator model (1). These geometric concepts are illustrated in Figure 4 for the two-dimensional case.

[1]For example, in power network applications the coupling terms $a_{ij} \sin(\theta_i - \theta_j)$ are power flows along transmission lines $\{i,j\} \in \mathcal{E}$, and the phase distances $|\theta_i - \theta_j|$ are bounded well below $\pi/2$ due to thermal constraints. In Subsection III-D, we present a converse synchronization notion, where the goal is to maximize phase distances.

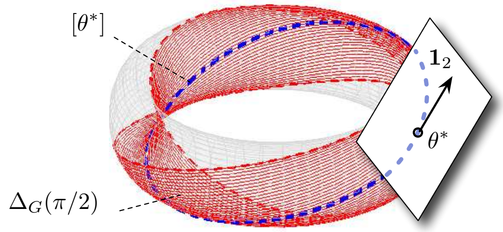

Fig. 4. Illustration of the state space $\mathbb{T}^2$, the set $\Delta_G(\pi/2)$, the synchronization manifold $[\theta^*]$ associated to a phase-synchronized angle array $\theta^* = (\theta_1^*, \theta_2^*) \in \bar{\Delta}_G(0)$, and the tangent space with translation vector $\mathbf{1}_2$ at θ^*.

At this point, the interested reader should go through the exercise of analyzing a simple network of two oscillators, which illustrates the basic synchronization phenomenology and the different synchronization notions, see [75].

B. Synchronization Metrics

The notion of phase cohesiveness can be understood as a performance measure for synchronization and phase synchronization is simply the extreme case of phase cohesiveness with $\lim_{t\to\infty} \theta(t) \in \bar{\Delta}_G(0) = \overline{\text{Arc}}_n(0)$. An alternative performance measure is the magnitude of the so-called *order parameter* introduced by Kuramoto [6], [7]:

$$re^{\mathrm{i}\psi} = \frac{1}{n} \sum\nolimits_{j=1}^n e^{\mathrm{i}\theta_j} .$$

The order parameter is the centroid of all oscillators represented as points on the unit circle in $\mathbb{C}$. The magnitude r of the order parameter is a synchronization measure: if all oscillators are phase-synchronized, then $r = 1$, and if all oscillators are spaced equally on the unit circle, then $r = 0$. The latter case is characterized in Subsection III-D. For a complete graph, the magnitude r of the order parameter serves as an *average* performance index for synchronization, and phase cohesiveness can be understood as a *worst-case* performance index. Extensions of the order parameter tailored to non-complete graphs have been proposed in [20], [53], [57].

For a complete graph and for γ sufficiently small, the set $\bar{\Delta}_G(\gamma)$ reduces to $\overline{\text{Arc}}_n(\gamma)$, the arc of length γ containing all oscillators. The order parameter is contained within the convex hull of this arc since it is the centroid of all oscillators, see Figure 5. In this case, the magnitude r of the order parameter can be related to the arc length γ.

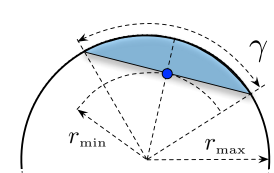

Fig. 5. Schematic illustration of an arc of length $\gamma \in [0, \pi]$, its convex hull (shaded), and the value ● of the corresponding order parameter $re^{\mathrm{i}\psi}$ with minimum magnitude $r_{\text{min}} = \cos(\gamma/2)$ and maximum magnitude $r_{\text{max}} = 1$.

Lemma 3.1: (**Shortest arc length and order parameter, [75, Lemma 2.1]**) Given an angle array $\theta = (\theta_1, \ldots, \theta_n) \in \mathbb{T}^n$ with $n \geq 2$, let $r(\theta) = \frac{1}{n} |\sum_{j=1}^n e^{\mathrm{i}\theta_j}|$ be the magnitude of the order parameter, and let $\gamma(\theta)$ be the length of the shortest arc containing all angles, that is, $\theta \in \overline{\text{Arc}}_n(\gamma(\theta))$. The following statements hold:

1) if $\gamma(\theta) \in [0, \pi]$, then $r(\theta) \in [\cos(\gamma(\theta)/2), 1]$; and
2) if $\theta \in \overline{\text{Arc}}_n(\pi)$, then $\gamma(\theta) \in [2\arccos(r(\theta)), \pi]$.

C. Synchronization Conditions

The coupled oscillator dynamics (1) feature (i) the synchronizing coupling described by the graph $G(\mathcal{V}, \mathcal{E}, A)$ and (ii) the de-synchronizing effect of the non-uniform natural frequencies ω. Loosely speaking, synchronization occurs when the coupling dominates the non-uniformity. Various conditions have been proposed to quantify this trade-off.

The coupling is typically quantified by the algebraic connectivity $\lambda_2(L)$ [45], [46], [53], [65], [124], [125] or the weighted nodal degree $\deg_i \triangleq \sum_{j=1}^{n} a_{ij}$ [65], [97], [114], [126], [127], and the non-uniformity is quantified by either absolute norms $\|\omega\|_p$ or incremental norms $\|B^T\omega\|_p$, where typically $p \in \{2, \infty\}$. Sometimes, these conditions can be evaluated only numerically since they are state-dependent [124], [126] or arise from a non-trivial linearization process, such as the Master stability function formalism [45], [46], [128]. In general, concise and accurate results are known only for specific topologies such as complete graphs [75], linear chains [107], and bipartite graphs [83] with uniform weights.

For arbitrary coupling topologies only sufficient conditions are known [53], [65], [124], [126] as well as numerical investigations for random networks [90], [98], [125], [129]. Simulation studies indicate that these conditions are conservative estimates on the threshold from incoherence to synchrony. Literally, every review article on synchronization draws attention to the problem of finding sharp synchronization conditions [4], [8], [9], [45]–[47], [75].

D. Phase Balancing and Splay State

In certain applications in neuroscience [12]–[14], deep-brain stimulation [27], [28], and vehicle coordination [20], [29]–[32], one is not interested in the coherent behavior with synchronized phases, but rather in the phenomenon of synchronized frequencies and de-sychronized phases.

Whereas the phase-synchronized state is characterized by the order parameter r achieving its maximal (unit) magnitude, we say that a solution $\theta : \mathbb{R}_{\geq 0} \to \mathbb{T}^n$ to the coupled oscillator model (1) achieves *phase balancing* if all phases $\theta_i(t)$ converge to $\text{Bal}_n = \{\theta \in \mathbb{T}^n : r(\theta) = |\frac{1}{n}\sum_{j=1}^{n} e^{\mathrm{i}\theta_j}| = 0\}$ as $t \to \infty$, that is, the oscillators are distributed over the unit circle $\mathbb{S}^1$, such that their centroid $re^{\mathrm{i}\psi}$ vanishes.

One balanced state of particular interest in neuroscience applications is the so-called *splay state* corresponding to phases uniformly distributed around the unit circle $\mathbb{S}^1$ with distances $2\pi/n$. Other highly symmetric balanced states consist of multiple clusters of collocated phases, where the clusters themselves are arranged in splay state, see [29], [30].

IV. Analysis of Synchronization

In this section we present several analysis approaches to synchronization in the coupled oscillator model (1). We begin with a few basic ideas to provide important intuition as well as the analytic basis for further analysis.

A. Some Simple Yet Important Insights

The potential energy $U : \mathbb{T}^n \to \mathbb{R}$ of the elastic spring network in Figure 1 is, up to an additive constant, given by

$$U(\theta) = \sum\nolimits_{\{i,j\}\in\mathcal{E}} a_{ij}\big(1 - \cos(\theta_i - \theta_j)\big)\,. \tag{9}$$

By means of the potential energy, the coupled oscillator model (1) can reformulated as the forced gradient system

$$\dot\theta_i = \omega_i - \nabla_i U(\theta)\,, \qquad i \in \{1, \dots, n\}\,, \tag{10}$$

where $\nabla_i U(\theta) = \frac{\partial}{\partial\theta_i} U(\theta)$ denotes the partial derivative. It can be easily verified that the phase-synchronized state $\theta_i = \theta_j$ for all $\{i, j\} \in \mathcal{E}$ is a local minimum of the potential energy (9). The gradient formulation (10) clearly emphasizes the competition between the synchronization-enforcing coupling through the potential $U(\theta)$ and the synchronization-inhibiting heterogeneous natural frequencies ω_i.

We next note that ω has to be bounded, relative to the nodal degree, in order for a synchronized solution to exist.

Lemma 4.1: **(Necessary sync conditions)** Consider the coupled oscillator model (1) with graph $G(\mathcal{V}, \mathcal{E}, A)$, frequencies $\omega \in \mathbf{1}_n^\perp$, and nodal degree $\deg_i = \sum_{j=1}^{n} a_{ij}$ for each oscillator $i \in \{1, \dots, n\}$. If there exists a synchronized solution $\theta \in \bar\Delta_G(\gamma)$ for some $\gamma \in [0, \pi/2]$, then the following conditions hold:

1) **Absolute bound:** For each node $i \in \{1, \dots, n\}$,
$$\deg_i \sin(\gamma) \geq |\omega_i|\,; \tag{11}$$
2) **Incremental bound:** For all distinct $i, j \in \{1, \dots, n\}$,
$$(\deg_i + \deg_j)\sin(\gamma) \geq |\omega_i - \omega_j|\,. \tag{12}$$

Proof: Since $\omega \in \mathbf{1}_n^\perp$, the synchronization frequency ω_{sync} is zero, and phase and frequency synchronized solutions are equilibrium solutions determined by the equations

$$\omega_i = \sum\nolimits_{j=1}^{n} a_{ij}\sin(\theta_i - \theta_j)\,, \qquad i \in \{1, \dots, n\}\,. \tag{13}$$

Since $\sin(\theta_i - \theta_j) \in [-\sin(\gamma), +\sin(\gamma)]$ for $\theta \in \bar\Delta_G(\gamma)$, the equilibrium equations (13) have no solution if condition (11) is not satisfied. Since $\omega \in \mathbf{1}_n^\perp$, an incremental bound on ω seems to be more appropriate than an absolute bound. The subtraction of the ith and jth equation (13) yields

$$\omega_i - \omega_j = \sum\nolimits_{k=1}^{n} \left(a_{ik}\sin(\theta_i - \theta_k) - a_{jk}\sin(\theta_j - \theta_k)\right)\,.$$

Again, since the coupling is bounded, the above equation has no solution in $\bar\Delta_G(\gamma)$ if condition (12) is not satisfied. ∎

The following result is fundamental for various analysis approaches synchronization. To the best of the authors' knowledge this result has been first established in [130].

Lemma 4.2: (**Stable synchronization in** $\Delta_G(\pi/2)$) Consider the coupled oscillator model (1) with a connected graph $G(\mathcal{V}, \mathcal{E}, A)$ and $\omega \in \mathbf{1}_n^\perp$. The following statements hold:

1) **Jacobian:** The Jacobian $J(\theta)$ of the coupled oscillator model (1) evaluated at $\theta \in \mathbb{T}^n$ is given by
$$J(\theta) = -B\,\text{diag}(\{a_{ij}\cos(\theta_i - \theta_j)\}_{\{i,j\}\in\mathcal{E}})B^T\,;$$
2) **Local stability and uniqueness:** If there exists an equilibrium $\theta^* \in \Delta_G(\pi/2)$, then

(i) $-J(\theta^*)$ is a Laplacian matrix;

(ii) the equilibrium manifold $[\theta^*] \in \Delta_G(\pi/2)$ is locally exponentially stable; and

(iii) this equilibrium manifold is unique in $\bar{\Delta}_G(\pi/2)$.

Proof: Since $\frac{\partial}{\partial\theta_i}\big(\omega_i - \sum_{j=1}^n a_{ij}\sin(\theta_i - \theta_j)\big) = -\sum_{j=1}^n a_{ij}\cos(\theta_i - \theta_j)$ and $\frac{\partial}{\partial\theta_j}\big(\omega_i - \sum_{j=1}^n a_{ij}\sin(\theta_i - \theta_j)\big) = a_{ij}\cos(\theta_i - \theta_j)$, we obtain that the Jacobian is equal to minus the Laplacian matrix of the connected graph $G(\mathcal{V},\mathcal{E},\tilde{A})$ with the (possibly negative) weights $\tilde{a}_{ij} = a_{ij}\cos(\theta_i - \theta_j)$. Equivalently, $J(\theta) = -B\,\mathrm{diag}(\{a_{ij}\cos(\theta_i - \theta_j)\}_{\{i,j\}\in\mathcal{E}})B^T$. This completes the proof of statement 1).

The Jacobian $J(\theta)$ evaluated for an equilibrium $\theta^* \in \Delta_G(\pi/2)$ is minus the Laplacian matrix of the graph $G(\mathcal{V},\mathcal{E},\tilde{A})$ with strictly positive weights $\tilde{a}_{ij} = a_{ij}\cos(\theta_i^* - \theta_j^*) > 0$ for every $\{i,j\} \in \mathcal{E}$. Hence, $J(\theta^*)$ is negative semidefinite with the nullspace $\mathbf{1}_n$ arising from the rotational symmetry, see Figure 4. Consequently, the equilibrium point $\theta^* \in \Delta_G(\pi/2)$ is locally (transversally) exponentially stable, or equivalently, the corresponding equilibrium manifold $[\theta^*] \in \Delta_G(\pi/2)$ is locally exponentially stable.

The uniqueness statement follows since the right-hand side of the coupled oscillator model (1) is a one-to-one function (modulo rotational symmetry) for $\theta \in \bar{\Delta}_G(\pi/2)$, see [131, Corollary 1]. This completes the proof of statement 2). ■

By Lemma 4.2, any equilibrium in $\Delta_G(\pi/2)$ is stable which supports the notion of phase cohesiveness as a performance metric. Since the Jacobian $J(\theta)$ is the negative Hessian of the potential $U(\theta)$ defined in (9), Lemma 4.2 implies that any equilibrium in $\Delta_G(\pi/2)$ is a local minimizer of $U(\theta)$. Of particular interest are so-called $\mathbb{S}^1$*-synchronizing graphs* for which all critical points of (9) are hyperbolic, the phase-synchronized state is the global minimum of $U(\theta)$, and all other critical points are local maxima or saddle points. The class of $\mathbb{S}^1$-synchronizing graphs includes, among others, complete graphs and acyclic graphs [99]–[102].

These basic insights motivated various characterizations and explorations of the critical points and the curvature of the potential $U(\theta)$ in the literature on synchronization [53], [65], [75], [90], [99], [99]–[102], [102] as well as on power systems [62], [113], [124], [126], [130]–[133].

B. Phase Synchronization

If all natural frequencies are identical, $\omega_i \equiv \omega$ for all $i \in \{1,\dots,n\}$, then a transformation of the coupled oscillator model (1) to a rotating frame with frequency ω leads to

$$\dot{\theta}_i = -\sum_{j=1}^n a_{ij}\sin(\theta_i - \theta_j)\,, \qquad i \in \{1,\dots,n\}\,. \quad (14)$$

The analysis of the coupled oscillator model (14) is particularly simple and local phase synchronization can be concluded by various analysis methods. A sample of different methods (by far not complete) includes the contraction property [55], [65], [93], [99], [134], quadratic Lyapunov functions [53], [65], linearization [82], [102], or order parameter and potential function arguments [29], [57], [81].

The following theorem on phase synchronization summarizes a collection of results originally presented in [29], [55], [57], [75], [99], [102], and it can be easily proved given the insights developed in Subsection IV-A.

Theorem 4.3: **(Phase synchronization)** Consider the coupled oscillator model (1) with a connected graph $G(\mathcal{V},\mathcal{E},A)$ and with frequency $\omega \in \mathbb{R}^n$ (not necessarily zero mean). The following statements are equivalent:

(i) **Stable phase sync:** there exists a locally exponentially stable phase-synchronized solution $\theta \in \overline{\mathrm{Arc}}_n(0)$ (or a synchronization manifold $[\theta] \in \bar{\Delta}_G(0)$); and

(ii) **Uniformity:** there exists a constant $\omega \in \mathbb{R}$ such that $\omega_i = \omega$ for all $i \in \{1,\dots,n\}$.

If the two equivalent cases (i) and (ii) are true, the following statements hold:

1) **Global convergence:** For all initial angles $\theta(0) \in \mathbb{T}^n$ all frequencies $\dot{\theta}_i(t)$ converge to ω and all phases $\theta_i(t) - \omega t \pmod{2\pi}$ converge to the critical points $\{\theta \in \mathbb{T}^n : \nabla U(\theta) = \mathbf{0}_n\}$;
2) **Semi-global stability:** The region of attraction of the phase-synchronized solution $\theta \in \overline{\mathrm{Arc}}_n(0)$ contains the open semi-circle $\mathrm{Arc}_n(\pi)$, and each arc $\overline{\mathrm{Arc}}_n(\gamma)$ is positively invariant for every arc length $\gamma < \pi$;
3) **Explicit phase:** For initial angles in an open semi-circle $\theta(0) \in \mathrm{Arc}_n(\pi)$, the asymptotic synchronization phase is given by[2] $\theta(t) = \sum_{i=1}^n \theta_i(0)/n + \omega t \pmod{2\pi}$;
4) **Convergence rate:** For every initial angle $\theta(0) \in \overline{\mathrm{Arc}}_n(\gamma)$ with $\gamma < \pi$, the exponential convergence rate to phase synchronization is no worse than $\lambda_{\text{ps}} = -\lambda_2(L)\,\mathrm{sinc}(\gamma)$; and
5) **Almost global stability:** If the graph $G(\mathcal{V},\mathcal{E},A)$ is $\mathbb{S}^1$-synchronizing, the region of attraction of the phase-synchronized solution $\theta \in \overline{\mathrm{Arc}}_n(0)$ is almost all of $\mathbb{T}^n$.

Proof: Implication (i) $\Longrightarrow$ (ii): By assumption, there exist constants $\theta_{\text{sync}} \in \mathbb{S}^1$ and $\omega_{\text{sync}} \in \mathbb{R}$ such that $\theta_i(t) = \theta_{\text{sync}} + \omega_{\text{sync}} t \pmod{2\pi}$. In the phase-synchronized case, the dynamics (1) then read as $\omega_{\text{sync}} = \omega_i$ for all $i \in \{1,\dots,n\}$. Hence, a necessary condition for the existence of phase synchronization is that all ω_i are identical.

Implication (ii) $\Longrightarrow$ (i): Consider the model (1) written in a rotating frame with frequency ω as in (14). Note that the set of phase-synchronized solutions $\bar{\Delta}_G(0)$ is an equilibrium manifold. By Lemma 4.2, we conclude that $\bar{\Delta}_G(0)$ is locally exponentially stable. This concludes the proof of (i) ⇔ (ii).

Statement 1): Note that (14) can be written as the gradient flow $\dot{\theta} = -\nabla U(\theta)$, and the corresponding potential function $U(\theta)$ is non-increasing along trajectories. Since the sublevel sets of $U(\theta)$ are compact and the vector field $\nabla U(\theta)$ is smooth, the invariance principle [135, Theorem 4.4] asserts that every solution converges to set of equilibria of (14).

Statements 2): The coupled oscillator model (14) can be re-written as the consensus-type system

$$\dot{\theta}_i = -\sum_{j=1}^n b_{ij}(\theta)\cdot(\theta_i - \theta_j)\,, \qquad i \in \{1,\dots,n\}\,, \quad (15)$$

where the weights $b_{ij}(\theta) = a_{ij}\,\mathrm{sinc}(\theta_i - \theta_j)$ depend explicitly on the system state. Notice that for $\theta \in \overline{\mathrm{Arc}}_n(\gamma)$

[2] This "average" of angles (points on $\mathbb{S}^1$) is well-defined in an open semi-circle. If the parametrization of θ has no discontinuity inside the arc containing all angles, then the average can be obtained by the usual formula.

and $\gamma < \pi$ the weights $b_{ij}(\theta)$ are upper and lower bounded as $b_{ij}(\theta) \in [a_{ij}\,\text{sinc}(\gamma), a_{ij}]$ Assume that the initial angles $\theta_i(0)$ belong to the set $\overline{\text{Arc}}_n(\gamma)$, that is, they are all contained in an arc of length $\gamma \in [0, \pi[$. In this case, a natural Lyapunov function to establish phase synchronization can be obtained from the *contraction property*, which aims at showing that the convex hull containing all oscillators is decreasing, see [55], [65], [93], [99], [136] and the review [134, Section 2].

Recall the geodesic distance between two angles on $\mathbb{S}^1$ and define the continuous function $V : \mathbb{T}^n \to [0, \pi]$ by

$$V(\psi) = \max\{|\psi_i - \psi_j| \mid i, j \in \{1, \dots, n\}\}. \tag{16}$$

Notice that, if all angles are contained in an arc at time t, then the arc length $V(\theta(t)) = \max_{i,j\in\{1,\dots,n\}} |\theta_i(t) - \theta_j(t)|$ is a Lyapunov function candidate for phase synchronization. Indeed, it can be shown that $V(\theta(t))$ decreases for $\theta(0) \in \overline{\text{Arc}}_n(\gamma)$ and for all $\gamma < \pi$. The analysis is complicated by the following fact: the function $V(\theta(t))$ is continuous but not necessarily differentiable when the maximum geodesic distance (the right-hand side of (16)), is attained by more than one pair of oscillators. We omit the explicit calculations here and refer to [55], [65], [75], [84], [93] for details.

Statement 3): By statement 2), the set $\text{Arc}_n(\pi)$ is positively invariant, and for $\theta(0) \in \text{Arc}_n(\pi)$ the average $\sum_{i=1}^{n} \theta_i(t)/n$ is well defined for $t \geq 0$. A summation over all equations of the model (14) yields $\sum_{i=1}^{n} \dot{\theta}_i(t) = 0$, or equivalently, $\sum_{i=1}^{n} \theta_i(t)$ is constant for all $t \geq 0$. In particular, for $t = 0$ we have that $\sum_{i=1}^{n} \theta_i(t) = \sum_{i=1}^{n} \theta_i(0)$ and for a phase-synchronized solution we have that $\sum_{i=1}^{n} \theta_{\text{sync}} = \sum_{i=1}^{n} \theta_i(0)$. Hence, the explicit synchronization phase is given by $\sum_{i=1}^{n} \theta_i(0)/n$. In the original coordinates (non-rotating frame) the synchronization phase is given by $\sum_{i=1}^{n} \theta_i(0)/n + \omega t \pmod{2\pi}$.

Statement 4): Given the invariance of the set $\overline{\text{Arc}}_n(\gamma)$ for any $\gamma < \pi$, the system (15) can be analyzed as a linear time-varying consensus system with initial condition $\theta(0) \in \overline{\text{Arc}}_n(\gamma)$, and bounded time-varying weights $b_{ij}(\theta(t)) \in [a_{ij}\,\text{sinc}(\gamma), a_{ij}]$ for all $t \geq 0$. The worst-case convergence rate λ_{ps} can then be obtained by a standard symmetric consensus analysis, see [53], [54], [65], [75]. For instance, it can be shown that the deviation of the angles $\theta(t)$ from their average, $\|\theta(t) - (\sum_{i=1}^{n} \theta(t)/n)\mathbf{1}_n\|_2^2$ (the *disagreement function*) decays exponentially with rate λ_{ps}.

Statement 5): By statement 1), all solutions of system (14) converge to the set of equilibria, which equals the set of critical points of the potential $U(\theta)$. By the definition of $\mathbb{S}^1$-synchronizing graphs, the phase-synchronized equilibrium manifold $\overline{\text{Arc}}_n(0)$ is the only stable equilibrium set, and all others are unstable. Hence, for all initial condition $\theta(0) \in \mathbb{T}^n$, which are not on the stable manifolds of unstable equilibria, the corresponding solution $\theta(t)$ will reach the phase-synchronized equilibrium manifold $\overline{\text{Arc}}_n(0)$. ■

Remark 2: (**Control-theoretic perspective on synchronization)** As established in Theorem 4.3, the set of phase-synchronized solutions $\overline{\text{Arc}}_n(0)$ of the coupled oscillator model (1) is locally stable provided that all natural frequencies are identical. For non-uniform (but sufficiently identical) natural frequencies, phase synchronization is not possible but a certain degree of phase cohesiveness can still be achieved. Hence, the coupled oscillator model (1) can be regarded as an exponentially stable system subject to the disturbance $\omega \in \mathbf{1}_n^\perp$, and classic control-theoretic concepts such as input-to-state stability, practical stability, and ultimate boundedness [135] or their incremental versions [137] can be used to study synchronization. In control-theoretic terminology, synchronization and phase cohesiveness can then also be described as "practical phase synchronization". Compared to prototypical nonlinear control examples, various additional challenges arise in the analysis of the coupled oscillator model (1) due to the bounded and non-monotone sinusoidal coupling and the compact state space $\mathbb{T}^n$ containing numerous equilibria; see the analysis approaches in Section IV and [65], [75], [95].□

C. Phase Balancing

In general, only few results are known about the phase balancing problem. This asymmetry is partially caused by the fact that phase synchrony is required in more applications than phase balancing. Moreover, the phase-synchronized set $\overline{\text{Arc}}_n(0)$ admits a very simple geometric characterization, whereas the phase-balanced set Bal_n has a complicated geometric structure [29]. Moreover, Bal_n consists of numerous disjoint subsets, and the number of these subsets grows with the number of nodes n in a combinatorial fashion.

Consider the coupled oscillator model (14) with identical natural frequencies. By inverting the direction of time, we get

$$\dot{\theta}_i = \sum\nolimits_{j=1}^{n} a_{ij} \sin(\theta_i - \theta_j)\,, \qquad i \in \{1, \dots, n\}\,. \tag{17}$$

In the following, we say that the interaction graph $G(\mathcal{V}, \mathcal{E}, A)$ is *circulant* if the adjacency matrix $A = A^T$ is a circulant matrix. Circulant graphs are highly symmetric graphs including complete graphs, bipartite graphs, and ring graphs.For circulant graphs, the coupled oscillator model (17) achieves phase balancing. The following theorem summarizes different results, which were originally presented in [29], [30].

Theorem 4.4: **(Phase balancing)** Consider the coupled oscillator model (17) with uniformly weighted and circulant graph $G(\mathcal{V}, \mathcal{E}, A)$. The following statements hold:

1) **Local phase balancing:** The phase-balanced set Bal_n is locally asymptotically stable; and
2) **Almost global stability:** If the graph $G(\mathcal{V}, \mathcal{E}, A)$ is complete, then the region of attraction of the stable phase-balanced set Bal_n is almost all of $\mathbb{T}^n$.

The proof of Theorem 4.4 follows a similar reasoning as the proof of Theorem 4.3: convergence is established by potential function arguments and local (in)stability of equilibria by Jacobian arguments. We omit the proof here and refer to [29, Theorem 1] and [30, Theorem 2] for details.

For general connected graphs, the conclusions of Theorem 4.4 are not true. As a remedy to achieve locally stable and globally attractive phase balancing, higher order models need to be considered, see the models proposed in [30], [57].

D. Synchronization in Complete Networks

For a complete coupling graph with uniform weights $a_{ij} = K/n$, where $K > 0$ is the *coupling gain*, the coupled oscillator model (1) reduces to the celebrated Kuramoto model

$$\dot{\theta}_i = \omega_i - \frac{K}{n}\sum\nolimits_{j=1}^{n} \sin(\theta_i - \theta_j)\,, \qquad i \in \{1,\dots,n\}\,. \quad (18)$$

By means of the order parameter $re^{\mathrm{i}\psi} = \frac{1}{n}\sum_{j=1}^{n} e^{\mathrm{i}\theta_j}$, the Kuramoto model (18) can be rewritten in the insightful form

$$\dot{\theta}_i = \omega_i - Kr\sin(\theta_i - \psi)\,, \quad i \in \{1,\dots,n\}\,. \qquad (19)$$

Equation (19) gives the intuition that the oscillators synchronize by coupling to a mean field represented by the order parameter $re^{\mathrm{i}\psi}$. Intuitively, for small coupling strength K each oscillator rotates with its natural frequency ω_i, whereas for large K all angles $\theta_i(t)$ will be entrained by the mean field $re^{\mathrm{i}\psi}$ and synchronize. The threshold from incoherence to synchrony occurs for some critical coupling K_{critical}. This phase transition has been the source of numerous investigations starting with Kuramoto's analysis [6], [7]. Various necessary, sufficient, implicit, and explicit estimates of K_{critical} for both the on-set as well as the ultimate stage of synchronization have been proposed [6]–[9], [29], [53], [54], [65], [75], [76], [83]–[88], [95]–[97], [99], [102]–[106], [109], and we refer to [75] for a comprehensive overview.

The mean field approach to the equations (19) can be made mathematically rigorous by a time-scale separation [96] or in the continuum limit as the number of oscillators tends to infinity and the natural frequencies ω are sampled from a distribution function $g : \mathbb{R} \to \mathbb{R}_{\geq 0}$. In the continuum limit and for a symmetric, continuous, and unimodal distribution $g(\omega)$, Kuramoto himself showed in an insightful and ingenuous analysis [6], [7] that the incoherent state (a uniform distribution of the oscillators on the unit circle $\mathbb{S}^1$) supercritically bifurcates for the critical coupling strength

$$K_{\text{critical}} = \frac{2}{\pi g(0)}\,. \qquad (20)$$

In [9], [88], [103], it was found that the bipolar (bimodal double-delta) distribution (respectively the uniform distribution) yield the largest (respectively smallest) threshold K_{critical} over all distributions $g(\omega)$ with bounded support. We refer [8], [9] for further references and to [89], [108], [109] for recent contributions on the continuum limit model.

In the finite-dimensional case, the necessary synchronization condition (12) gives a lower bound for K_{critical} as

$$K \geq \frac{n}{2(n-1)} \cdot (\omega_{\max} - \omega_{\min})\,. \qquad (21)$$

Three recent articles [85]–[87] independently derived a set of implicit consistency equations for the *exact* critical coupling strength K_{critical} for which synchronized solutions exist. Verwoerd and Mason provided the following implicit formulae to compute K_{critical} [87, Theorem 3]:

$$\begin{aligned} &K_{\text{critical}} = nu^* \Big/ \sum\nolimits_{i=1}^{n} \sqrt{1-(\Omega_i/u^*)^2}\,, \\ &2\sum\nolimits_{i=1}^{n} \sqrt{1-(\Omega_i/u^*)^2} = \sum\nolimits_{i=1}^{n} 1\Big/\sqrt{1-(\Omega_i/u^*)^2}, \end{aligned} \qquad (22)$$

where $\Omega_i = \omega_i - \omega_{\text{sync}}$ and $u^* \in [\|\Omega\|_\infty, 2\|\Omega\|_\infty]$. The implicit formulae (22) can also be extended to bipartite graphs [83]. A local stability analysis is carried out in [85], [86].

From the point of analyzing or designing a sufficiently strong coupling, the exact formulae (22) have three drawbacks. First, they are implicit and thus not suited for performance or robustness estimates in case of additional coupling strength for a given $K > K_{\text{critical}}$. Second, the corresponding region of attraction of a synchronized solution is unknown. Third and finally, the particular natural frequencies ω_i are typically time-varying, uncertain, or even unknown in the applications listed in Section I. In this case, the exact value of K_{critical} needs to be estimated in continuous time, or a conservatively strong coupling $K \gg K_{\text{critical}}$ has to be chosen.

The following theorem states an explicit bound on the critical coupling together with performance estimates and a guaranteed semi-global region of attraction. This bound is necessary and sufficient when considering arbitrary distributions of the natural frequencies with compact support. The result has been originally presented in [75, Theorem 4.1].

Theorem 4.5: **(Synchronization in the Kuramoto model)** Consider the Kuramoto model (18) with natural frequencies $\omega = (\omega_1,\dots,\omega_n)$ and coupling strength K. The following three statements are equivalent:

(i) the coupling strength K is larger than the maximum non-uniformity among the natural frequencies, that is,

$$K > K_{\text{critical}} \triangleq \omega_{\max} - \omega_{\min}\,; \qquad (23)$$

(ii) there exists an arc length $\gamma_{\max} \in \,]\pi/2, \pi]$ such that the Kuramoto model (18) synchronizes exponentially for all possible distributions of the natural frequencies ω_i supported on the compact interval $[\omega_{\min}, \omega_{\max}]$ and for all initial phases $\theta(0) \in \mathrm{Arc}_n(\gamma_{\max})$; and

(iii) there exists an arc length $\gamma_{\min} \in [0, \pi/2[$ such that the Kuramoto model (18) has a locally exponentially stable synchronization manifold in $\overline{\mathrm{Arc}}_n(\gamma_{\min})$ for all possible distributions of the natural frequencies ω_i supported on the compact interval $[\omega_{\min}, \omega_{\max}]$.

If the three equivalent conditions (i), (ii), and (iii) hold, then the ratio K_{critical}/K and the arc lengths $\gamma_{\min} \in [0, \pi/2[$ and $\gamma_{\max} \in \,]\pi/2, \pi]$ are related uniquely via $\sin(\gamma_{\min}) = \sin(\gamma_{\max}) = K_{\text{critical}}/K$, and the following statements hold:

1) **phase cohesiveness:** the set $\overline{\mathrm{Arc}}_n(\gamma) \subseteq \bar{\Delta}_G(\gamma)$ is positively invariant for every $\gamma \in [\gamma_{\min}, \gamma_{\max}]$, and each trajectory starting in $\mathrm{Arc}_n(\gamma_{\max})$ approaches asymptotically $\overline{\mathrm{Arc}}_n(\gamma_{\min})$;
2) **frequency synchronization:** the asymptotic synchronization frequency is the average frequency $\omega_{\text{sync}} = \frac{1}{n}\sum_{i=1}^{n}\omega_i$, and, given phase cohesiveness in $\overline{\mathrm{Arc}}_n(\gamma)$ for some fixed $\gamma < \pi/2$, the exponential synchronization rate is no worse than $\lambda_{\mathrm{K}} = -K\cos(\gamma)$; and
3) **order parameter:** the asymptotic value of the magnitude of the order parameter, denoted by $r_\infty \triangleq \lim_{t\to\infty} \frac{1}{n}|\sum_{j=1}^{n} e^{\mathrm{i}\theta_j(t)}|$, is bounded as

$$1 \geq r_\infty \geq \cos\Big(\frac{\gamma_{\min}}{2}\Big) = \sqrt{\frac{1+\sqrt{1-(K_{\text{critical}}/K)^2}}{2}}\,.$$

Proof: In the following, we sketch the proof of Theorem 4.5 and refer to [75, Theorem 4.1] for further details.

Implication (i) $\Longrightarrow$ (ii): In a first step, it is shown that the phase cohesive set $\overline{\mathrm{Arc}}_n(\gamma)$ is positively invariant for every $\gamma \in [\gamma_{\min}, \gamma_{\max}]$. By assumption, the angles $\theta_i(t)$ belong to the set $\overline{\mathrm{Arc}}_n(\gamma)$ at time $t = 0$. We aim to show that all angles remain in $\overline{\mathrm{Arc}}_n(\gamma)$ for all $t > 0$ by means of the contraction Lyapunov function (16). Note that $\overline{\mathrm{Arc}}_n(\gamma)$ is positively invariant if and only if $V(\theta(t))$ does not increase at any time t such that $V(\theta(t)) = \gamma$. The *upper Dini derivative* of $V(\theta(t))$ along trajectories of (18) is given by

$$D^+V(\theta(t)) = \limsup_{h \downarrow 0} \frac{V(\theta(t+h)) - V(\theta(t))}{h} .$$

Written out in components and after trigonometric simplifications [75], we obtain that the derivative is bounded as

$$D^+V(\theta(t)) \leq \omega_{\max} - \omega_{\min} - K\sin(\gamma) .$$

It follows that the length of the arc formed by the angles is non-increasing in $\overline{\mathrm{Arc}}_n(\gamma)$ if and only if

$$K\sin(\gamma) \geq K_{\text{critical}} , \tag{24}$$

where K_{critical} is as stated in equation (23). For $\gamma \in [0,\pi]$ the left-hand side of (24) is a concave function of γ that achieves its maximum at $\gamma^* = \pi/2$. Therefore, there exists an open set of arc lengths $\gamma \in [0,\pi]$ satisfying equation (24) if and only if equation (24) is true with the strict equality sign at $\gamma^* = \pi/2$, which corresponds to condition (23). Additionally, if these two equivalent statements are true, then there exists a unique $\gamma_{\min} \in [0, \pi/2[$ and a $\gamma_{\max} \in]\pi/2, \pi]$ that satisfy equation (24) with the equality sign, namely $\sin(\gamma_{\min}) = \sin(\gamma_{\max}) = K_{\text{critical}}/K$. For every $\gamma \in [\gamma_{\min}, \gamma_{\max}]$ it follows that the arc-length $V(\theta(t))$ is non-increasing, and it is strictly decreasing for $\gamma \in]\gamma_{\min}, \gamma_{\max}[$. Among other things, this shows that statement (i) implies statement 1). By means of Lemma 3.1, statement 3) then follows from statement 1).

The frequency dynamics of the Kuramoto model (18) can be obtained by differentiating the Kuramoto model (18) as

$$\frac{d}{dt}\,\dot\theta_i = \sum\nolimits_{j=1}^{n} \tilde a_{ij}(t)\,(\dot\theta_j - \dot\theta_i) , \tag{25}$$

where $\tilde a_{ij}(t) = (K/n)\cos(\theta_i(t) - \theta_j(t))$. For $K > K_{\text{critical}}$, we just proved that for every $\theta(0) \in \mathrm{Arc}_n(\gamma_{\max})$ and for all $\gamma \in]\gamma_{\min}, \gamma_{\max}[$ there exists a finite time $T \geq 0$ such that $\theta(t) \in \overline{\mathrm{Arc}}_n(\gamma)$ for all $t \geq T$. Consequently, the terms $\tilde a_{ij}(t)$ are strictly positive for all $t \geq T$. Notice also that system (25) evolves on the tangent space of $\mathbb{T}^n$, that is, the Euclidean space $\mathbb{R}^n$. Now fix $\gamma \in]\gamma_{\min}, \pi/2[$ and let $T \geq 0$ such that $\tilde a_{ij}(t) > 0$ for all $t \geq T$. In this case, the frequency dynamics (25) can be analyzed as linear time-varying consensus system. By standard consensus arguments [49]–[51], it follows that $\|\dot\theta - \omega_{\text{sync}}\mathbf{1}_n\| \leq \|\dot\theta(0) - \omega_{\text{sync}}\mathbf{1}_n\| e^{-\lambda_{\kappa} t}$ for all $t \geq T$. This proves statement 2) and the implication (i) $\Longrightarrow$ (ii).

Implication (ii) $\Longrightarrow$ (i): To show that condition (23) is also necessary, it suffices to construct a counter example for which $K \leq K_{\text{critical}}$ and the oscillators do not achieve frequency synchronization even though all $\omega_i \in [\omega_{\min}, \omega_{\max}]$ and $\theta(0) \in \mathrm{Arc}_n(\gamma)$ for every $\gamma \in]\pi/2, \pi]$. Consider a bipolar distribution of the natural frequencies. Let the index set $\{1, \dots, n\}$ be partitioned by the two non-empty sets $\mathcal{I}_1$ and $\mathcal{I}_2$. Let $\omega_i = \omega_{\min}$ for $i \in \mathcal{I}_1$ and $\omega_i = \omega_{\max}$ for $i \in \mathcal{I}_2$, and assume that at some time $t \geq 0$ it holds that $\theta_i(t) = -\gamma/2$ for $i \in \mathcal{I}_1$ and $\theta_i(t) = +\gamma/2$ for $i \in \mathcal{I}_2$ and for some $\gamma \in [0, \pi[$. By construction, at time t all oscillators are contained in an arc of length $\gamma \in [0,\pi[$. Assume now that $K < K_{\text{critical}}$ and the oscillators synchronize. It can be shown [75] that the evolution of the arc length $V(\theta(t))$ satisfies the *equality*

$$D^+V(\theta(t)) = \omega_{\max} - \omega_{\min} - K\sin(\gamma) . \tag{26}$$

Clearly, for $K < K_{\text{critical}}$ the arc length $V(\theta(t)) = \gamma$ is increasing for any $\gamma \in [0,\pi]$. Thus, the phases are not bounded in $\overline{\mathrm{Arc}}_n(\gamma)$. This contradicts the assumption that the oscillators synchronize for $K < K_{\text{critical}}$ from every initial condition $\theta(0) \in \overline{\mathrm{Arc}}_n(\gamma)$. For $K = K_{\text{critical}}$, we know from [85], [86] that phase-locked equilibria have a zero eigenvalue with a two-dimensional Jacobian block, and thus synchronization cannot occur. This instability via a two-dimensional Jordan block is also visible in (26) since $D^+V(\theta(t))$ is increasing for $\theta(t) \in \overline{\mathrm{Arc}}_n(\gamma)$, $\gamma \in]\pi/2, \pi]$ until all oscillators change orientation. This proves the implication (ii) $\Longrightarrow$ (i).

Equivalence (i),(ii) $\Leftrightarrow$ (iii): The proof relies on Jacobian arguments and will be omitted here, see [75] for details. ■

Theorem 4.5 places a hard bound on the critical coupling strength K_{critical} for all distributions of ω_i supported on the compact interval $[\omega_{\min}, \omega_{\max}]$. For a particular distribution $g(\omega)$ supported on $[\omega_{\min}, \omega_{\max}]$ the bound (23) is only sufficient and possibly a factor 2 larger than the necessary bound (21). The exact critical coupling lies somewhere in between and can be obtained from the implicit equations (22).

Since the bound (23) on K_{critical} is exact [75] for the worst-case bipolar distribution $\omega_i \in \{\omega_{\min}, \omega_{\max}\}$, Figure 6 reports numerical findings for the other extreme case [88] of a uniform distribution $g(\omega) = 1/2$ supported for $\omega_i \in [-1, 1]$. All three displayed bounds are identical for $n = 2$ oscillators. As n increases, the sufficient bound (23) converges to the width $\omega_{\max} - \omega_{\min} = 2$ of the support of $g(\omega)$, and the necessary bound (21) accordingly to half of the width. The exact bound (22) converges to $4(\omega_{\max} - \omega_{\min})/(2\pi) = 4/\pi$ in agreement with condition (20) predicted for the continuum limit.

Finally, we remark that that Theorem 4.5 can be extended to time-varying natural frequencies [75], and, for a particular sampling distribution $g(\omega)$, the critical quantity $\omega_{\max} - \omega_{\min}$ can be estimated by extreme value statistics, see [90].

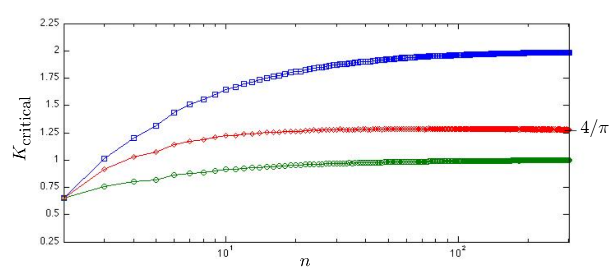

Fig. 6. Statistical analysis of the necessary and explicit bound (21) (◇), the exact and implicit bound (22) (○), and the sufficient, tight, and explicit bound (23) (□) for $n \in [2, 300]$ oscillators in a semi-log plot, where the coupling gains for each n are averaged over 1000 simulations.

E. Synchronization in Sparse Networks

As summarized in Subsection III-C, the quest for sharp and concise synchronization for non-complete coupling graph $G(\mathcal{V}, \mathcal{E}, A)$ is an important and outstanding problem emphasized in every review article on coupled oscillator networks [8], [9], [45]–[47], [75]. The approaches known for phase synchronization in arbitrary graphs or the contraction approach to frequency synchronization (used in the proof of Theorem 4.5) do not generally extend to arbitrary natural frequencies $\omega \in \mathbf{1}_n^\perp$ and connected coupling graphs $G(\mathcal{V}, \mathcal{E}, A)$, or do so only under extremely conservative conditions.

One Lyapunov function advocated for classic Kuramoto oscillators (18) is the function $W : \mathrm{Arc}_n(\pi) \to \mathbb{R}$ defined for angles θ in an open semi-circle and given by [53], [54]

$$W(\theta) = \frac{1}{4} \sum\nolimits_{i,j=1}^{n} |\theta_i - \theta_j|^2 = \frac{1}{2} \left\| B_c^T \theta \right\|_2^2 , \qquad (27)$$

where $B_c \in \mathbb{R}^{n \times (n(n-1)/2)}$ is an incidence matrix of the complete graph. As shown in [65, Theorem 4.4], the Lyapunov function (27) generalizes also to the coupled oscillator model (1). Indeed, an even more general model is considered in [65], and a Lyapunov analysis yields the following result.

Theorem 4.6: **(Frequency synchronization I)** Consider the coupled oscillator model (1) with a connected graph $G(\mathcal{V}, \mathcal{E}, A)$ and $\omega \in \mathbf{1}_n^\perp$. Assume that the algebraic connectivity is larger than a critical value, that is,

$$\lambda_2(L) > \lambda_{\text{critical}} \triangleq \left\| B_c^T \omega \right\|_2 , \qquad (28)$$

where $B_c \in \mathbb{R}^{n \times n(n-1)/2}$ is the incidence matrix of the complete graph. Accordingly, define $\gamma_{\max} \in \,]\pi/2, \pi]$ and $\gamma_{\min} \in [0, \pi/2[$ as unique solutions to $(\pi/2) \cdot \mathrm{sinc}(\gamma_{\max}) = \sin(\gamma_{\min}) = \lambda_{\text{critical}}/\lambda_2(L)$. The following statements hold:

1) **phase cohesiveness:** the set $\{\theta \in \mathrm{Arc}_n(\pi) : \|B_c^T \theta\|_2 \leq \gamma\} \subseteq \bar{\Delta}_G(\gamma)$ is positively invariant for every $\gamma \in [\gamma_{\min}, \gamma_{\max}]$, and each trajectory starting in the set $\{\theta \in \mathrm{Arc}_n(\pi) : \|B_c^T \theta\|_2 < \gamma_{\max}\}$ asymptotically reaches the set $\{\theta \in \mathrm{Arc}_n(\pi) : \|B_c^T \theta\|_2 \leq \gamma_{\min}\}$; and
2) **frequency synchronization:** for every $\theta(0) \in \mathrm{Arc}_n(\pi)$ with $\|B_c^T \theta(0)\|_2 < \gamma_{\max}$ the frequencies $\dot{\theta}_i(t)$ synchronize exponentially to the average frequency $\omega_{\text{sync}} = \frac{1}{n} \sum_{i=1}^{n} \omega_i$, and, given phase cohesiveness in $\bar{\Delta}_G(\gamma)$ for some fixed $\gamma < \pi/2$, the exponential synchronization rate is no worse than $\lambda_{\text{fe}} = -\lambda_2(L) \cos(\gamma)$.

The proof of Theorem 4.6 follows a similar ultimate-boundedness strategy as the proof of Theorem 4.5 by using the 2-norm type Lyapunov function (27). The proof can be found in the extended version of this paper [138].

For classic Kuramoto oscillators (18), condition (28) reduces to $K > \|B_c^T \omega\|_2$. Clearly, the condition $K > \|B_c^T \omega\|_2$ is more conservative than the bound (23) which reads as $K > \|B_c^T \omega\|_\infty = \omega_{\max} - \omega_{\min}$. One reason for this conservatism is that the analysis leading to condition (28) requires *all* phase distances $|\theta_i - \theta_j|$ to be bounded, whereas according to Lemma 4.2 only *pairwise* phase distances $|\theta_i - \theta_j|$, $\{i, j\} \in \mathcal{E}$, need to be bounded for stable synchronization. The following result exploits these weaker assumptions and states a sharper (but only local) synchronization condition.

Theorem 4.7: **(Frequency synchronization II)** Consider the coupled oscillator model (1) with a connected graph $G(\mathcal{V}, \mathcal{E}, A)$ and $\omega \in \mathbf{1}_n^\perp$. There exists a locally exponentially stable equilibrium manifold $[\theta] \in \Delta_G(\pi/2)$ if

$$\lambda_2(L) > \left\| B^T \omega \right\|_2 . \qquad (29)$$

Moreover, if condition (29) holds, then $[\theta]$ is phase cohesive in $\{\theta \in \mathbb{T}^n : \|B^T \theta\|_2 \leq \gamma_{\min}\} \subseteq \bar{\Delta}_G(\gamma_{\min})$, where $\gamma_{\min} \in [0, \pi/2[$ satisfies $\sin(\gamma_{\min}) = \|B^T \omega\|_2 / \lambda_2(L)$.

The strategy to prove Theorem 4.7 is inspired by the ingenuous analysis in [53, Section IIV.B]. It relies on the insight gained from Lemma 4.2 that any synchronization manifold $[\theta] \in \Delta_G(\pi/2)$ is locally stable, and it formulates the existence of such a synchronization manifold as a fixed point problem. Here, we follow the basic proof strategy in [53], but we provide a more accurate result together. The proof is reported in the extended version of this paper [138].

V. Conclusions and Open Research Directions

In this paper we introduced the reader to the coupled oscillator model (1), we reviewed several applications, we discussed different synchronization notions, and we presented different analysis approaches to synchronization.

Despite the vast literature, the countless applications, and the numerous theoretic results on the synchronization properties of model (1), many interesting and important problems are still open. In the following, we summarize limitations of the existing analysis approaches and present a few worthwhile directions for future research.

First, in many applications the coupling between the oscillators is not purely sinusoidal. For instance, phase delays in neuroscience [14], time delays in sensor networks [38], or transfer conductances in power networks [64] lead to a "shifted coupling" of the form $\sin(\theta_i - \theta_j - \varphi_{ij})$, where $\varphi_{ij} \in [-\pi/2, \pi/2]$. In this case and also for other "skewed" or "symmetry-breaking" coupling functions, many of the presented analysis schemes either fail or lead to overly conservative results. Another interesting class of oscillator networks are pulse-coupled oscillators featuring impulsive coupling at discrete time instants. Pulse-coupled oscillators admit a very interesting phenomenology [139], and most results known for continuously-coupled oscillators still need to be extended to pulse-coupled oscillators.

Second, in many applications [13], [25], [35], [64], [68] the coupled oscillator dynamics are not given by a simple first-order phase model of the form (1). Rather, the dynamics are of higher order, or sometimes there is no readily available phase variable to describe the limit cycle attracting the coupled dynamics. The analysis of oscillator networks with more general oscillator dynamics is largely unexplored. Whereas advances have been made for the simple case of phase synchronization of linear or passive oscillator networks, the case of frequency synchronization of non-identical oscillators with higher-order dynamics is not well-studied.

Third, despite the vast scientific interest the quest for sharp, concise, and closed-form synchronization conditions for arbitrary complex graphs has been so far in vain [8], [9], [45]–[47], [75]. As suggested by Lemma 4.1, Lemma

4.2, and Theorem 4.5, the proper metric for the synchronization problem is the incremental ∞-norm $\|B^T\theta\|_\infty = \max_{\{i,j\}\in\mathcal{E}} |\theta_i - \theta_j|$. In the authors' opinion, an analysis of the coupled oscillator model (1) with the incremental ∞-norm will likely deliver the sharpest possible conditions. However, such an analysis is very challenging for arbitrary natural frequencies $\omega \in \mathbf{1}_n^\perp$ and connected and weighted coupling graphs $G(\mathcal{V},\mathcal{E},A)$. Recent work [4] by the authors puts forth a novel algebraic condition for synchronization with a rigorous analysis for specific classes of graphs and with (only) a statistical validation for generic weighted graphs.

Fourth and finally, a few interesting and open theoretical challenges include the following. First, most of the presented analysis approaches and conditions do not extend to time-varying or directed coupling graphs $G(\mathcal{V},\mathcal{E},A)$, and alternative methods need to be developed. Second, most known estimates on the region of attraction of a synchronized solution are conservative. The semi-circle estimates given in Theorem 4.3 and Theorem 4.5 are conservative. We refer to [64], [110] for a set of interesting results and conjectures on the region of attraction. Third, the presented analysis approaches are restricted to synchronized equilibria inside $\Delta_G(\pi/2)$. Other interesting equilibrium configurations outside $\Delta_G(\pi/2)$ include splay state equilibria or frequency-synchronized equilibria with phases spread over an entire semi-circle.

We sincerely hope that this tutorial article stimulates further exciting research on synchronization in coupled oscillators, both on the theoretical side as well as in the countless applications.

References

[1] C. Huygens, *Horologium Oscillatorium*, Paris, France, 1673.

[2] S. H. Strogatz, *SYNC: The Emerging Science of Spontaneous Order*. Hyperion, 2003.

[3] A. T. Winfree, *The Geometry of Biological Time*, 2nd ed. Springer, 2001.

[4] F. Dörfler, M. Chertkov, and F. Bullo, "Synchronization in complex oscillator networks and smart grids," Jul. 2012, available at http://arxiv.org/abs/1208.0045.

[5] A. T. Winfree, "Biological rhythms and the behavior of populations of coupled oscillators," *Journal of Theoretical Biology*, vol. 16, no. 1, pp. 15–42, 1967.

[6] Y. Kuramoto, "Self-entrainment of a population of coupled nonlinear oscillators," in *Int. Symposium on Mathematical Problems in Theoretical Physics*, ser. Lecture Notes in Physics, H. Araki, Ed. Springer, 1975, vol. 39, pp. 420–422.

[7] ——, *Chemical Oscillations, Waves, and Turbulence*. Springer, 1984.

[8] S. H. Strogatz, "From Kuramoto to Crawford: Exploring the onset of synchronization in populations of coupled oscillators," *Physica D: Nonlinear Phenomena*, vol. 143, no. 1, pp. 1–20, 2000.

[9] J. A. Acebrón, L. L. Bonilla, C. J. P. Vicente, F. Ritort, and R. Spigler, "The Kuramoto model: A simple paradigm for synchronization phenomena," *Reviews of Modern Physics*, vol. 77, no. 1, pp. 137–185, 2005.

[10] D. C. Michaels, E. P. Matyas, and J. Jalife, "Mechanisms of sinoatrial pacemaker synchronization: a new hypothesis," *Circulation Research*, vol. 61, no. 5, pp. 704–714, 1987.

[11] C. Liu, D. R. Weaver, S. H. Strogatz, and S. M. Reppert, "Cellular construction of a circadian clock: period determination in the suprachiasmatic nuclei," *Cell*, vol. 91, no. 6, pp. 855–860, 1997.

[12] F. Varela, J. P. Lachaux, E. Rodriguez, and J. Martinerie, "The brainweb: Phase synchronization and large-scale integration," *Nature Reviews Neuroscience*, vol. 2, no. 4, pp. 229–239, 2001.

[13] E. Brown, P. Holmes, and J. Moehlis, "Globally coupled oscillator networks," in *Perspectives and Problems in Nonlinear Science: A Celebratory Volume in Honor of Larry Sirovich*, E. Kaplan, J. E. Marsden, and K. R. Sreenivasan, Eds. Springer, 2003, pp. 183–215.

[14] S. M. Crook, G. B. Ermentrout, M. C. Vanier, and J. M. Bower, "The role of axonal delay in the synchronization of networks of coupled cortical oscillators," *Journal of Computational Neuroscience*, vol. 4, no. 2, pp. 161–172, 1997.

[15] A. K. Ghosh, B. Chance, and E. K. Pye, "Metabolic coupling and synchronization of NADH oscillations in yeast cell populations," *Archives of Biochemistry and Biophysics*, vol. 145, no. 1, pp. 319–331, 1971.

[16] J. Buck, "Synchronous rhythmic flashing of fireflies. II." *Quarterly Review of Biology*, vol. 63, no. 3, pp. 265–289, 1988.

[17] T. J. Walker, "Acoustic synchrony: two mechanisms in the snowy tree cricket," *Science*, vol. 166, no. 3907, pp. 891–894, 1969.

[18] N. Kopell and G. B. Ermentrout, "Coupled oscillators and the design of central pattern generators," *Mathematical Biosciences*, vol. 90, no. 1-2, pp. 87–109, 1988.

[19] N. E. Leonard, T. Shen, B. Nabet, L. Scardovi, I. D. Couzin, and S. A. Levin, "Decision versus compromise for animal groups in motion," *Proceedings of the National Academy of Sciences*, vol. 109, no. 1, pp. 227–232, 2012.

[20] D. A. Paley, N. E. Leonard, R. Sepulchre, D. Grunbaum, and J. K. Parrish, "Oscillator models and collective motion," *IEEE Control Systems Magazine*, vol. 27, no. 4, pp. 89–105, 2007.

[21] Z. Néda, E. Ravasz, T. Vicsek, Y. Brechet, and A.-L. Barabási, "Physics of the rhythmic applause," *Physical Review E*, vol. 61, no. 6, pp. 6987–6992, 2000.

[22] H. Daido, "Quasientrainment and slow relaxation in a population of oscillators with random and frustrated interactions," *Physical Review Letters*, vol. 68, no. 7, pp. 1073–1076, 1992.

[23] G. Jongen, J. Anemüller, D. Bollé, A. C. C. Coolen, and C. Perez-Vicente, "Coupled dynamics of fast spins and slow exchange interactions in the XY spin glass," *Journal of Physics A: Mathematical and General*, vol. 34, no. 19, pp. 3957–3984, 2001.

[24] J. Pantaleone, "Stability of incoherence in an isotropic gas of oscillating neutrinos," *Physical Review D*, vol. 58, no. 7, p. 073002, 1998.

[25] K. Wiesenfeld, P. Colet, and S. H. Strogatz, "Frequency locking in Josephson arrays: Connection with the Kuramoto model," *Physical Review E*, vol. 57, no. 2, pp. 1563–1569, 1998.

[26] I. Z. Kiss, Y. Zhai, and J. L. Hudson, "Emerging coherence in a population of chemical oscillators," *Science*, vol. 296, no. 5573, pp. 1676–1678, 2002.

[27] P. A. Tass, "A model of desynchronizing deep brain stimulation with a demand-controlled coordinated reset of neural subpopulations," *Biological Cybernetics*, vol. 89, no. 2, pp. 81–88, 2003.

[28] A. Nabi and J. Moehlis, "Single input optimal control for globally coupled neuron networks," *Journal of Neural Engineering*, vol. 8, p. 065008, 2011.

[29] R. Sepulchre, D. A. Paley, and N. E. Leonard, "Stabilization of planar collective motion: All-to-all communication," *IEEE Transactions on Automatic Control*, vol. 52, no. 5, pp. 811–824, 2007.

[30] ——, "Stabilization of planar collective motion with limited communication," *IEEE Transactions on Automatic Control*, vol. 53, no. 3, pp. 706–719, 2008.

[31] D. J. Klein, "Coordinated control and estimation for multi-agent systems: Theory and practice," Ph.D. dissertation, University of Washington, 2008.

[32] D. J. Klein, P. Lee, K. A. Morgansen, and T. Javidi, "Integration of communication and control using discrete time Kuramoto models for multivehicle coordination over broadcast networks," *IEEE Journal on Selected Areas in Communications*, vol. 26, no. 4, pp. 695–705, 2008.

[33] M. M. U. Rahman, R. Mudumbai, and S. Dasgupta, "Consensus based carrier synchronization in a two node network," in *IFAC World Congress*, Milan, Italy, Aug. 2011, pp. 10 038–10 043.

[34] G. Kozyreff, A. G. Vladimirov, and P. Mandel, "Global coupling with time delay in an array of semiconductor lasers," *Physical Review Letters*, vol. 85, no. 18, pp. 3809–3812, 2000.

[35] F. C. Hoppensteadt and E. M. Izhikevich, "Synchronization of laser oscillators, associative memory, and optical neurocomputing," *Physical Review E*, vol. 62, no. 3, pp. 4010–4013, 2000.

[36] R. A. York and R. C. Compton, "Quasi-optical power combining using mutually synchronized oscillator arrays," *IEEE Transactions on Microwave Theory and Techniques*, vol. 39, no. 6, pp. 1000–1009, 2002.

[37] W. C. Lindsey, F. Ghazvinian, W. C. Hagmann, and K. Dessouky, "Network synchronization," *Proceedings of the IEEE*, vol. 73, no. 10, pp. 1445–1467, 1985.

[38] O. Simeone, U. Spagnolini, Y. Bar-Ness, and S. H. Strogatz, "Distributed synchronization in wireless networks," *IEEE Signal Processing Magazine*, vol. 25, no. 5, pp. 81–97, 2008.

[39] Y. W. Hong and A. Scaglione, "A scalable synchronization protocol for large scale sensor networks and its applications," *IEEE Journal on Selected Areas in Communications*, vol. 23, no. 5, pp. 1085–1099, 2005.

[40] R. Baldoni, A. Corsaro, L. Querzoni, S. Scipioni, and S. T. Piergiovanni, "Coupling-based internal clock synchronization for large-scale dynamic distributed systems," *IEEE Transactions on Parallel and Distributed Systems*, vol. 21, no. 5, pp. 607–619, 2010.

[41] Y. Wang, F. Núñez, and F. J. Doyle, "Increasing sync rate of pulse-coupled oscillators via phase response function design: theory and application to wireless networks," *IEEE Transactions on Control Systems Technology*, 2012, to appear.

[42] E. Mallada and A. Tang, "Distributed clock synchronization: Joint frequency and phase consensus," in *IEEE Conf. on Decision and Control and European Control Conference*, Orlando, FL, USA, Dec. 2011, pp. 6742–6747.

[43] S. Barbarossa and G. Scutari, "Decentralized maximum-likelihood estimation for sensor networks composed of nonlinearly coupled dynamical systems," *IEEE Transactions on Signal Processing*, vol. 55, no. 7, pp. 3456–3470, 2007.

[44] J. W. Simpson-Porco, F. Dörfler, and F. Bullo, "Droop-controlled inverters are Kuramoto oscillators," in *IFAC Workshop on Distributed Estimation and Control in Networked Systems*, Santa Barbara, CA, USA, Sep. 2012, pp. 264–269.

[45] A. Arenas, A. Díaz-Guilera, J. Kurths, Y. Moreno, and C. Zhou, "Synchronization in complex networks," *Physics Reports*, vol. 469, no. 3, pp. 93–153, 2008.

[46] S. Boccaletti, V. Latora, Y. Moreno, M. Chavez, and D. U. Hwang, "Complex networks: Structure and dynamics," *Physics Reports*, vol. 424, no. 4-5, pp. 175–308, 2006.

[47] S. H. Strogatz, "Exploring complex networks," *Nature*, vol. 410, no. 6825, pp. 268–276, 2001.

[48] J. A. K. Suykens and G. V. Osipov, "Introduction to focus issue: Synchronization in complex networks," *Chaos*, vol. 18, no. 3, pp. 037 101–037 101, 2008.

[49] R. Olfati-Saber, J. A. Fax, and R. M. Murray, "Consensus and cooperation in networked multi-agent systems," *Proceedings of the IEEE*, vol. 95, no. 1, pp. 215–233, 2007.

[50] W. Ren, R. W. Beard, and E. M. Atkins, "Information consensus in multivehicle cooperative control: Collective group behavior through local interaction," *IEEE Control Systems Magazine*, vol. 27, no. 2, pp. 71–82, 2007.

[51] F. Bullo, J. Cortés, and S. Martínez, *Distributed Control of Robotic Networks*. Princeton University Press, 2009.

[52] L. Moreau, "Stability of multiagent systems with time-dependent communication links," *IEEE Transactions on Automatic Control*, vol. 50, no. 2, pp. 169–182, 2005.

[53] A. Jadbabaie, N. Motee, and M. Barahona, "On the stability of the Kuramoto model of coupled nonlinear oscillators," in *American Control Conference*, Boston, MA, USA, Jun. 2004, pp. 4296–4301.

[54] N. Chopra and M. W. Spong, "On exponential synchronization of Kuramoto oscillators," *IEEE Transactions on Automatic Control*, vol. 54, no. 2, pp. 353–357, 2009.

[55] Z. Lin, B. Francis, and M. Maggiore, "State agreement for continuous-time coupled nonlinear systems," *SIAM Journal on Control and Optimization*, vol. 46, no. 1, pp. 288–307, 2007.

[56] A. Sarlette and R. Sepulchre, "Consensus optimization on manifolds," *SIAM Journal on Control and Optimization*, vol. 48, no. 1, pp. 56–76, 2009.

[57] L. Scardovi, A. Sarlette, and R. Sepulchre, "Synchronization and balancing on the N-torus," *Systems & Control Letters*, vol. 56, no. 5, pp. 335–341, 2007.

[58] R. Olfati-Saber, "Swarms on sphere: A programmable swarm with synchronous behaviors like oscillator networks," in *IEEE Conf. on Decision and Control*, San Diego, CA, USA, 2006, pp. 5060–5066.

[59] G. B. Ermentrout, "An adaptive model for synchrony in the firefly *pteroptyx malaccae*," *Journal of Mathematical Biology*, vol. 29, no. 6, pp. 571–585, 1991.

[60] S. Y. Ha, E. Jeong, and M. J. Kang, "Emergent behaviour of a generalized Viscek-type flocking model," *Nonlinearity*, vol. 23, no. 12, pp. 3139–3156, 2010.

[61] S. Ha, C. Lattanzio, B. Rubino, and M. Slemrod, "Flocking and synchronization of particle models," *Quarterly Applied Mathematics*, vol. 69, pp. 91–103, 2011.

[62] A. R. Bergen and D. J. Hill, "A structure preserving model for power system stability analysis," *IEEE Transactions on Power Apparatus and Systems*, vol. 100, no. 1, pp. 25–35, 1981.

[63] P. W. Sauer and M. A. Pai, *Power System Dynamics and Stability*. Prentice Hall, 1998.

[64] H.-D. Chiang, C. C. Chu, and G. Cauley, "Direct stability analysis of electric power systems using energy functions: Theory, applications, and perspective," *Proceedings of the IEEE*, vol. 83, no. 11, pp. 1497–1529, 1995.

[65] F. Dörfler and F. Bullo, "Synchronization and transient stability in power networks and non-uniform Kuramoto oscillators," *SIAM Journal on Control and Optimization*, vol. 50, no. 3, pp. 1616–1642, 2012.

[66] J. Pantaleone, "Synchronization of metronomes," *American Journal of Physics*, vol. 70, p. 992, 2002.

[67] S. H. Strogatz, D. M. Abrams, A. McRobie, B. Eckhardt, and E. Ott, "Theoretical mechanics: Crowd synchrony on the Millennium Bridge," *Nature*, vol. 438, no. 7064, pp. 43–44, 2005.

[68] M. Bennett, M. F. Schatz, H. Rockwood, and K. Wiesenfeld, "Huygens's clocks," *Proceedings: Mathematical, Physical and Engineering Sciences*, vol. 458, no. 2019, pp. 563–579, 2002.

[69] Y.-P. Choi, S.-Y. Ha, and S.-B. Yun, "Complete synchronization of Kuramoto oscillators with finite inertia," *Physica D*, vol. 240, no. 1, pp. 32–44, 2011.

[70] H. A. Tanaka, A. J. Lichtenberg, and S. Oishi, "Self-synchronization of coupled oscillators with hysteretic responses," *Physica D: Nonlinear Phenomena*, vol. 100, no. 3-4, pp. 279–300, 1997.

[71] ——, "First order phase transition resulting from finite inertia in coupled oscillator systems," *Physical Review Letters*, vol. 78, no. 11, pp. 2104–2107, 1997.

[72] H. Hong, G. S. Jeon, and M. Y. Choi, "Spontaneous phase oscillation induced by inertia and time delay," *Physical Review E*, vol. 65, no. 2, p. 026208, 2002.

[73] H. Hong, M. Y. Choi, J. Yi, and K. S. Soh, "Inertia effects on periodic synchronization in a system of coupled oscillators," *Physical Review E*, vol. 59, no. 1, p. 353, 1999.

[74] J. A. Acebrón, L. L. Bonilla, and R. Spigler, "Synchronization in populations of globally coupled oscillators with inertial effects," *Physical Review E*, vol. 62, no. 3, pp. 3437–3454, 2000.

[75] F. Dörfler and F. Bullo, "On the critical coupling for Kuramoto oscillators," *SIAM Journal on Applied Dynamical Systems*, vol. 10, no. 3, pp. 1070–1099, 2011.

[76] F. De Smet and D. Aeyels, "Partial entrainment in the finite Kuramoto–Sakaguchi model," *Physica D: Nonlinear Phenomena*, vol. 234, no. 2, pp. 81–89, 2007.

[77] R. Mirollo and S. H. Strogatz, "The spectrum of the partially locked state for the Kuramoto model," *Journal of Nonlinear Science*, vol. 17, no. 4, pp. 309–347, 2007.

[78] Y. L. Maistrenko, O. V. Popovych, and P. A. Tass, "Desynchronization and chaos in the Kuramoto model," in *Dynamics of Coupled Map Lattices and of Related Spatially Extended Systems*, ser. Lecture Notes in Physics, J.-R. Chazottes and B. Fernandez, Eds. Springer, 2005, vol. 671, pp. 285–306.

[79] R. Tönjes, "Pattern formation through synchronization in systems of nonidentical autonomous oscillators," Ph.D. dissertation, Universitäts Potsdam, Germany, 2007.

[80] O. V. Popovych, Y. L. Maistrenko, and P. A. Tass, "Phase chaos in coupled oscillators," *Physical Review E*, vol. 71, no. 6, p. 065201, 2005.

[81] J. Lunze, "Complete synchronization of Kuramoto oscillators," *Journal of Physics A: Mathematical and Theoretical*, vol. 44, p. 425102, 2011.

[82] E. Canale and P. Monzón, "Almost global synchronization of symmetric Kuramoto coupled oscillators," in *Systems Structure and Control*. InTech Education and Publishing, 2008, ch. 8, pp. 167–190.

[83] M. Verwoerd and O. Mason, "On computing the critical coupling coefficient for the Kuramoto model on a complete bipartite graph," *SIAM Journal on Applied Dynamical Systems*, vol. 8, no. 1, pp. 417–453, 2009.

[84] S.-Y. Ha, T. Ha, and J.-H. Kim, "On the complete synchronization of the Kuramoto phase model," *Physica D: Nonlinear Phenomena*, vol. 239, no. 17, pp. 1692–1700, 2010.

[85] R. E. Mirollo and S. H. Strogatz, "The spectrum of the locked state for the Kuramoto model of coupled oscillators," *Physica D: Nonlinear Phenomena*, vol. 205, no. 1-4, pp. 249–266, 2005.

[86] D. Aeyels and J. A. Rogge, "Existence of partial entrainment and stability of phase locking behavior of coupled oscillators," *Progress on Theoretical Physics*, vol. 112, no. 6, pp. 921–942, 2004.

[87] M. Verwoerd and O. Mason, "Global phase-locking in finite populations of phase-coupled oscillators," *SIAM Journal on Applied Dynamical Systems*, vol. 7, no. 1, pp. 134–160, 2008.

[88] G. B. Ermentrout, "Synchronization in a pool of mutually coupled oscillators with random frequencies," *Journal of Mathematical Biology*, vol. 22, no. 1, pp. 1–9, 1985.

[89] M. Verwoerd and O. Mason, "A convergence result for the Kuramoto model with all-to-all coupling," *SIAM Journal on Applied Dynamical Systems*, vol. 10, no. 3, pp. 906–920, 2011.

[90] J. C. Bronski, L. DeVille, and M. J. Park, "Fully synchronous solutions and the synchronization phase transition for the finite N Kuramoto model," Nov. 2011, available at `http://arxiv.org/abs/1111.5302`.

[91] J. A. Rogge and D. Aeyels, "Stability of phase locking in a ring of unidirectionally coupled oscillators," *Journal of Physics A*, vol. 37, pp. 11 135–11 148, 2004.

[92] L. DeVille, "Transitions amongst synchronous solutions for the stochastic Kuramoto model," *Nonlinearity*, vol. 25, no. 5, pp. 1–20, 2011.

[93] U. Münz, A. Papachristodoulou, and F. Allgöwer, "Consensus reaching in multi-agent packet-switched networks with non-linear coupling," *International Journal of Control*, vol. 82, no. 5, pp. 953–969, 2009.

[94] L. Scardovi, "Clustering and synchronization in phase models with state dependent coupling," in *IEEE Conf. on Decision and Control*, Atlanta, GA, USA, Dec. 2010, pp. 627–632.

[95] A. Franci, A. Chaillet, and W. Pasillas-Lépine, "Existence and robustness of phase-locking in coupled Kuramoto oscillators under mean-field feedback," *Automatica*, vol. 47, no. 6, pp. 1193–1202, 2011.

[96] S. Y. Ha and M. Slemrod, "A fast-slow dynamical systems theory for the Kuramoto type phase model," *Journal of Differential Equations*, vol. 251, no. 10, pp. 2685–2695, 2011.

[97] L. Buzna, S. Lozano, and A. Diaz-Guilera, "Synchronization in symmetric bipolar population networks," *Physical Review E*, vol. 80, no. 6, p. 66120, 2009.

[98] Y. Moreno and A. F. Pacheco, "Synchronization of Kuramoto oscillators in scale-free networks," *Europhysics Letters*, vol. 68, p. 603, 2004.

[99] A. Sarlette, "Geometry and symmetries in coordination control," Ph.D. dissertation, University of Liège, Belgium, Jan. 2009.

[100] E. A. Canale, P. A. Monzón, and F. Robledo, "The wheels: an infinite family of bi-connected planar synchronizing graphs," in *IEEE Conf. Industrial Electronics and Applications*, Taichung, Taiwan, Jun. 2010, pp. 2204–2209.

[101] E. A. Canale, P. Monzón, and F. Robledo, "On the complexity of the classification of synchronizing graphs," in *Grid and Distributed Computing, Control and Automation*, Jeju Island, Korea, Dec. 2010, pp. 186–195.

[102] P. Monzón, "Almost global stability of dynamical systems," Ph.D. dissertation, Universidad de la República, Montevideo, Uruguay, Jul. 2006.

[103] J. L. van Hemmen and W. F. Wreszinski, "Lyapunov function for the Kuramoto model of nonlinearly coupled oscillators," *Journal of Statistical Physics*, vol. 72, no. 1, pp. 145–166, 1993.

[104] S. J. Chung and J. J. Slotine, "On synchronization of coupled Hopf-Kuramoto oscillators with phase delays," in *IEEE Conf. on Decision and Control*, Atlanta, GA, USA, Dec. 2010, pp. 3181–3187.

[105] G. S. Schmidt, U. Münz, and F. Allgöwer, "Multi-agent speed consensus via delayed position feedback with application to Kuramoto oscillators," in *European Control Conference*, Budapest, Hungary, Aug. 2009, pp. 2464–2469.

[106] E. Canale and P. Monzón, "On the characterization of families of synchronizing graphs for Kuramoto coupled oscillators," in *IFAC Workshop on Distributed Estimation and Control in Networked Systems*, Venice, Italy, Sep. 2009, pp. 42–47.

[107] S. H. Strogatz and R. E. Mirollo, "Phase-locking and critical phenomena in lattices of coupled nonlinear oscillators with random intrinsic frequencies," *Physica D: Nonlinear Phenomena*, vol. 31, no. 2, pp. 143–168, 1988.

[108] H. Chiba, "A proof of the Kuramoto's conjecture for a bifurcation structure of the infinite dimensional Kuramoto model," Aug. 2010, available at `http://arxiv.org/abs/1008.0249`.

[109] E. A. Martens, E. Barreto, S. H. Strogatz, E. Ott, P. So, and T. M. Antonsen, "Exact results for the Kuramoto model with a bimodal frequency distribution," *Physical Review E*, vol. 79, no. 2, p. 26204, 2009.

[110] D. A. Wiley, S. H. Strogatz, and M. Girvan, "The size of the sync basin," *Chaos*, vol. 16, no. 1, p. 015103, 2006.

[111] Y. Wang and F. J. Doyle, "On influences of global and local cues on the rate of synchronization of oscillator networks," *Automatica*, vol. 47, no. 6, pp. 1236–1242, 2011.

[112] E. W. Justh and P. S. Krishnaprasad, "Equilibria and steering laws for planar formations," *Systems & Control Letters*, vol. 52, no. 1, pp. 25–38, 2004.

[113] S. Sastry and P. Varaiya, "Hierarchical stability and alert state steering control of interconnected power systems," *IEEE Transactions on Circuits and Systems*, vol. 27, no. 11, pp. 1102–1112, 1980.

[114] F. Dörfler and F. Bullo, "Kron reduction of graphs with applications to electrical networks," *IEEE Transactions on Circuits and Systems I: Regular Papers*, vol. 60, no. 1, pp. 150–163, 2013.

[115] V. Fioriti, S. Ruzzante, E. Castorini, E. Marchei, and V. Rosato, "Stability of a distributed generation network using the Kuramoto models," in *Critical Information Infrastructure Security*, ser. Lecture Notes in Computer Science. Springer, 2009, pp. 14–23.

[116] G. Filatrella, A. H. Nielsen, and N. F. Pedersen, "Analysis of a power grid using a Kuramoto-like model," *The European Physical Journal B*, vol. 61, no. 4, pp. 485–491, 2008.

[117] M. Rohden, A. Sorge, M. Timme, and D. Witthaut, "Self-organized synchronization in decentralized power grids," *Physical Review Letters*, vol. 109, no. 6, p. 064101, 2012.

[118] D. Subbarao, R. Uma, B. Saha, and M. V. R. Phanendra, "Self-organization on a power system," *IEEE Power Engineering Review*, vol. 21, no. 12, pp. 59–61, 2001.

[119] D. J. Hill and G. Chen, "Power systems as dynamic networks," in *IEEE Int. Symposium on Circuits and Systems*, Kos, Greece, May 2006, pp. 722–725.

[120] F. C. Hoppensteadt and E. M. Izhikevich, *Weakly Connected Neural Networks*. Springer, 1997.

[121] E. M. Izhikevich, *Dynamical Systems in Neuroscience: The Geometry of Excitability and Bursting*. MIT Press, 2007.

[122] E. M. Izhikevich and Y. Kuramoto, "Weakly coupled oscillators," *Encyclopedia of Mathematical Physics*, vol. 5, p. 448, 2006.

[123] G. B. Ermentrout and N. Kopell, "Frequency plateaus in a chain of weakly coupled oscillators, I." *SIAM Journal on Mathematical Analysis*, vol. 15, no. 2, pp. 215–237, 1984.

[124] F. F. Wu and S. Kumagai, *Limits on Power Injections for Power Flow Equations to Have Secure Solutions*. Electronics Research Laboratory, College of Engineering, University of California, 1980.

[125] T. Nishikawa, A. E. Motter, Y. C. Lai, and F. C. Hoppensteadt, "Heterogeneity in oscillator networks: Are smaller worlds easier to synchronize?" *Physical Review Letters*, vol. 91, no. 1, p. 14101, 2003.

[126] F. Wu and S. Kumagai, "Steady-state security regions of power systems," *IEEE Transactions on Circuits and Systems*, vol. 29, no. 11, pp. 703–711, 1982.

[127] G. Korniss, M. B. Hastings, K. E. Bassler, M. J. Berryman, B. Kozma, and D. Abbott, "Scaling in small-world resistor networks," *Physics Letters A*, vol. 350, no. 5-6, pp. 324–330, 2006.

[128] L. M. Pecora and T. L. Carroll, "Master stability functions for synchronized coupled systems," *Physical Review Letters*, vol. 80, no. 10, pp. 2109–2112, 1998.

[129] J. Gómez-Gardeñes, Y. Moreno, and A. Arenas, "Paths to synchronization on complex networks," *Physical Review Letters*, vol. 98, no. 3, p. 34101, 2007.

[130] C. J. Tavora and O. J. M. Smith, "Stability analysis of power systems," *IEEE Transactions on Power Apparatus and Systems*, vol. 91, no. 3, pp. 1138–1144, 1972.

[131] A. Arapostathis, S. Sastry, and P. Varaiya, "Analysis of power-flow equation," *International Journal of Electrical Power & Energy Systems*, vol. 3, no. 3, pp. 115–126, 1981.

[132] C. J. Tavora and O. J. M. Smith, "Equilibrium analysis of power systems," *IEEE Transactions on Power Apparatus and Systems*, vol. 91, no. 3, pp. 1131–1137, 1972.

[133] M. Ilić, "Network theoretic conditions for existence and uniqueness of steady state solutions to electric power circuits," in *IEEE International Symposium on Circuits and Systems*, San Diego, CA, USA, May 1992, pp. 2821–2828.

[134] R. Sepulchre, A. Sarlette, and P. Rouchon, "Consensus in non-commutative spaces," in *IEEE Conf. on Decision and Control*, Atlanta, GA, USA, Dec. 2010, pp. 6596–6601.

[135] H. K. Khalil, *Nonlinear Systems*, 3rd ed. Prentice Hall, 2002.

[136] L. Moreau, "Stability of continuous-time distributed consensus algorithms," Feb. 2008, available at `http://arxiv.org/abs/math/0409010`.

[137] D. Angeli, "A Lyapunov approach to incremental stability properties," *IEEE Transactions on Automatic Control*, vol. 47, no. 3, pp. 410–421, 2002.

[138] F. Dörfler and F. Bullo, "Exploring synchronization in complex oscillator networks," Sep. 2012, Extended version including proofs. Available at `http://arxiv.org/abs/1209.1335`.

[139] A. Mauroy, "On the dichotomic collective behaviors of large populations of pulse-coupled firing oscillators," Ph.D. dissertation, University of Liège, Belgium, 2011.